Can lateral mobility be restored along a highly domesticated low-energy gravel-bed river?

Thomas Dépret, Nathalie Thommeret, Hervé Piégay, Emmanuèle Gautier

Can lateral mobility be restored along a highly domesticated low-energy gravel-bed river?

Thomas Dépret [a]*, Nathalie Thommeret [b], Hervé Piégay [c], Emmanuèle Gautier [d]

[a] Laboratoire de Géographie Physique, CNRS UMR8591, 2 rue Henri Dunant, 94320 Thiais, France

[b] Laboratoire Géomatique et Foncier, CNAM-ESGT, 1 Boulevard Pythagore, 72000 Le Mans, France

[c] Université de Lyon, CNRS, UMR 5600 - Environnement-Ville-Société, Site ENS de Lyon, 15 Parvis René Descartes, Lyon 69342, France

[d] Université Paris 1 Panthéon-Sorbonne, Laboratoire de Géographie Physique, CNRS UMR8591, 2 rue Henri Dunant, 94320 Thiais, France

* Corresponding author

Abstract

Fluvial engineering works such as weirs, rip-rap, groynes, and dykes have constrained for decades and more the lateral mobility of rivers, one of the key drivers of aquatic and riparian diversity. Preserving or restoring a sufficient space for river mobility has therefore become a major river management focus. Because the success and relevance of management actions are conditioned by the level of energy and sediment supply of rivers, such actions are generally considered unsuitable for low-energy rivers. However, some low-energy rivers have

numerous ancient engineering works along their length, especially bank protections, suggesting a potential capacity for bed migration. In this context, it is essential to determine to what extent planform dynamics is disturbed, and if lateral mobility can be restored. Herein, a case study was done on a 146 km stretch of the low-energy meandering gravel-bed Cher River (France). The goal of the study was to estimate the remnant shifting capacity, identify the factors controlling the location and intensity of lateral erosion, determine the potential for preserving and restoring lateral mobility, and examine management measures that could be implemented to this end. For that, field surveys, analysis of existing databases, aerial photographs, and laser imaging detection and ranging digital elevation model (LiDAR DEM) data were combined. The study revealed a strong longitudinal fragmentation of the river, with most of it laterally constrained due to the presence of anthropogenic structures such as bank protections, former gravel pits in the alluvial plain, bridges, and weirs. The river is now composed of a string of constrained and unconstrained reaches, and the space available for river shifting has been dramatically reduced. Due to these fluvial engineering works and anthropogenic legacies, the potential for lateral movement of the riverbed, and, therefore, diversification of riparian and aquatic habitats, is limited. Furthermore, lateral mobility could be preserved or restored only for very short sections of the river. It is therefore highly unlikely that good ecological status could be achieved on the entire river corridor through removal of bank protections. Nevertheless, a possible solution could be combining bank protection removals with a series of gravel augmentations close to each other.

Keywords

Lowland river; Erodible corridor; Anthropogenic constraints; Stream restoration; Meander migration; Ecological status

Highlights

- Potential for lateral mobility on a low-energy gravel bed river is estimated
- A strong decease in the shifting capacity due to anthropogenic constraints is found
- A short cumulative length of river along which the lateral mobility is still possible
- Good ecological status is not achievable on the entire river corridor even with rip-rap removal

1. Introduction

Due to their widespread presence on Earth, their tremendous attraction for human societies, and because their morphology reflects changes occurring from basin to reach scale, rivers are among the landscape units most influenced by anthropogenic constraints. In response to these constraints, river forms and processes have been heavily altered, causing homogenization of their aquatic and riparian habitats, degradation of their ecological quality, and impoverishment of the social and ecosystem services they provide (Basak et al., 2021; Borgwardt et al., 2019; Culhane et al., 2019; Dudgeon, 2019; Dudgeon et al., 2006; Ekka et al., 2020; Elosegi et al., 2010; Florsheim et al., 2008; Vörösmarty et al., 2010). Increasing awareness of this damage has led to attempts to mitigate the negative effects of these alterations, and an era of river repair has begun (Downs and Gregory, 2004; Fryirs and Brierley, 2016). Indeed, many countries have enacted legal frameworks aimed at protecting or improving the ecological status of rivers. One of the most striking examples is the Water Framework Directive (WFD), adopted in 2000 by the European Union, that commits member

states to achieve good ecological status of rivers, and to implement restoration measures to achieve this status (European Parliament and Council, 2000; Grizzeti et al., 2017).

From the Neolithic to the Middle-ages, anthropogenic constraints were mainly, if not exclusively, indirect, consisting of the modification of land cover in watersheds and floodplains, thereby affecting water and sediment fluxes and connectivity from hillslopes to rivers (Brown et al., 2018; Hoffmann, 2015; Hoffmann et al., 2010; Notebaert and Verstraeten, 2010). Over the last millennium, local constraints, most involving direct modification of river channels and acting at segment or reach scales, have strengthened, first with the development of weirs connected to mills from the 11th century, followed by the channelization and/or rectification of river courses from the 19th century, then the exponential installation of large dams and massive gravel mining areas in riverbeds and floodplains from the mid-20th century (Brown et al., 2018; Downs and Piegay, 2019; Lehner et al., 2011; Maas et al., 2021; Overeem et al., 2013; Rinaldi et al., 2005; Surian, 2021; Wohl, 2020). These local constraints have resulted in a dramatic loss of lateral mobility of rivers (Dépret et al., 2017; Fremier et al., 2014; Friedman et al., 1998; Reid and Church, 2015), even though lateral mobility is one of the main drivers of aquatic and riparian habitat diversity (Choné and Biron, 2016; Florsheim et al., 2008; Stanford et al., 2005; Tockner et al., 2010; Williams et al., 2020). For altered rivers, achieving good ecological status may be impossible without restoration of a sufficient space to allow rivers to move laterally.

Restoration of space for lateral movement is grounded on process-based principles through which rivers are believed to be able to self-restore, namely to recover fluvial landforms and functions, with minimal anthropogenic intervention (Beechie et al., 2010; Ciotti et al., 2021; Fryirs and Brierley, 2021). Self-restoration actions promote longitudinal and cross-wise topographic as well as grain size heterogeneity, which increases the diversity of habitats, particularly aquatic habitats (Gaeuman, 2012; Yarnell et al., 2006; Hauer et al., 2018;

Staenzel et al., 2020). Moreover, shifting riverscape mosaic processes guaranteed by the lateral mobility of rivers allow rejuvenation of riparian succession associated with pulse disturbance (e.g., Diaz-Redondo et al., 2018; Gonzalez del Tanago et al., 2021; Hauer et al., 2016; Stanford et al., 2005; Tockner et al., 2010). These approaches are especially relevant when natural lateral constraints and socio-economical issues (SEIs) in the floodplain are rare, and when river energy and bedload are high (Kondolf, 2011). Nonetheless, these approaches also could be appropriate for low-energy rivers, providing that the bed material is mobile and alluvial material is sufficiently erodible to allow such rivers to be inherently behaviourally sensitive (Fryirs, 2017).

At the reach scale, river mobility often is determined through reconstruction of planimetric trajectory evolution (Khan and Fryirs, 2020; Piégay et al., 2005; Reid and Brierley, 2015). For low-energy rivers, such methods can be unsuitable where lateral anthropogenic constraints occur that may block channel movement, causing channel responsiveness to be underestimated. Bank protection on such rivers often are not archived, and they may be difficult to determine in the field unless a careful survey of the bed is carried out at low flow (Dépret et al., 2017). Disentangling the natural and anthropogenic drivers responsible for the weak planform shifting of low-energy rivers may, therefore, be challenging. Such disentangling is yet crucial because it influences river responsiveness appraisal and the design of preservation or restoration strategies, acting on forms or processes, and depending on the trade-off between the timescale needed for recovery and the timescale desired by managers. Determining to what extent lateral mobility can be restored along highly domesticated low-energy gravel-bed rivers requires first examining if lateral processes are still active, and if so to what extent, and whether there is enough space for river shifting.

To answer these questions, a case study was done on a 146 km stretch of the Cher River (France), for which the long-term anthropogenic influence on planform displacements

as well as the potential for self-restoration of lateral dynamics have been demonstrated on several short discrete reaches (8–12 km) (Dépret et al., 2015, 2017, 2021; Vayssière et al., 2016, 2020). The aims of this study were to estimate the remnant shifting capacity, to identify the factors controlling the location and intensity of lateral erosion, to determine the potential for preservation and restoration of lateral mobility, and to examine the management measures that could be implemented to this end. Therefore, a methodological framework was developed combining (1) thorough field surveys and preexisting databases to identify the constraints on lateral mobility and the current SEIs in the floodplain; (2) geographic information systems (GIS) analysis aimed at reconstructing the planimetric evolutionary trajectory of the river from aerial photographs, to quantify the available space for river shifting with and without lateral constraints and/or SEIs, and to compute some of the main factors assumed to control retreat rates (specific stream power, curvature, lateral constraints, availability of the coarse bed-material load); and (3) statistical analysis to determine how these factors influence the occurrence and intensity of lateral erosion.

2. Characteristics of the study reach

After leaving its source at 713 m above sea level, the Cher River mainly flows through gorges across steep slopes or in deep valleys with a very narrow floodplain (upstream Cher in Figure 1). The upstream section of the river is located at the northwest end of the low-altitude mountainous Massif Central, which mainly consists of crystalline and metamorphic rocks (Larue, 1981, 2011). After 63 km, the Cher alluvial plain begins (Alluvial Cher in Figure 1) and the river becomes single thread with a meandering pattern developed over recent millennia (Vayssière et al., 2020). After first occupying the Tertiary graben of Montluçon, which continues for 45 km to the confluence with the Aumance River (Larue, 1981, 2011;

Simon-Coinçon et al., 2000), the river then crosses the sedimentary domain of the Parisian Basin, where it joins the Loire River at 38 m asl. The study reach extends over 146 km, between Montluçon at the beginning of the Alluvial Cher, and Vierzon at the junction with the Yèvre River, one of the main tributaries of the Cher River (Figure 1). With a surface median sediment diameter (D_{50}) of around 15–45 mm and a mean specific stream power of 20 W m^{-2} (calculated from the width of the active channel formed by flow channels and unvegetated bars) for a discharge not exceeded 99% of the time (close to bankfull discharge), it is a low-energy river with coarse gravel (Dépret, 2014; Dépret et al., 2015).

The alluvial infill is organized into two or three main stratigraphic levels. The base of the infill is composed of sand, gravel, and pebble, while the upper part consists of overflow deposits of clay, silt and sand (Dépret, 2014; Lablanche et al., 1994; Manivit et al., 1994; Larue, 1994; Turland et al., 1989c). A predominantly sandy layer is frequently interspersed between these two levels. Because of this composite structure and the coarse nature of the material, the banks are highly erodible (Dépret et al., 2015, 2017). Moreover, bed mobility occurs over several days per year (Dépret et al., 2015, 2017).

The rainfall-evaporation regime of the Cher is essentially influenced by western flows. High water occurs in winter, generally in February, and low water occurs in summer, typically in August. On the upstream part of the middle course of the river, the hydrological regime, in particular for low flow, is partly artificialized since the construction of the Rochebut Dam at the beginning of the 20th century. Along the 146 km stretch studied, along with the Aumance River, the Cher River receives contributions from one major tributary (Figure 1).

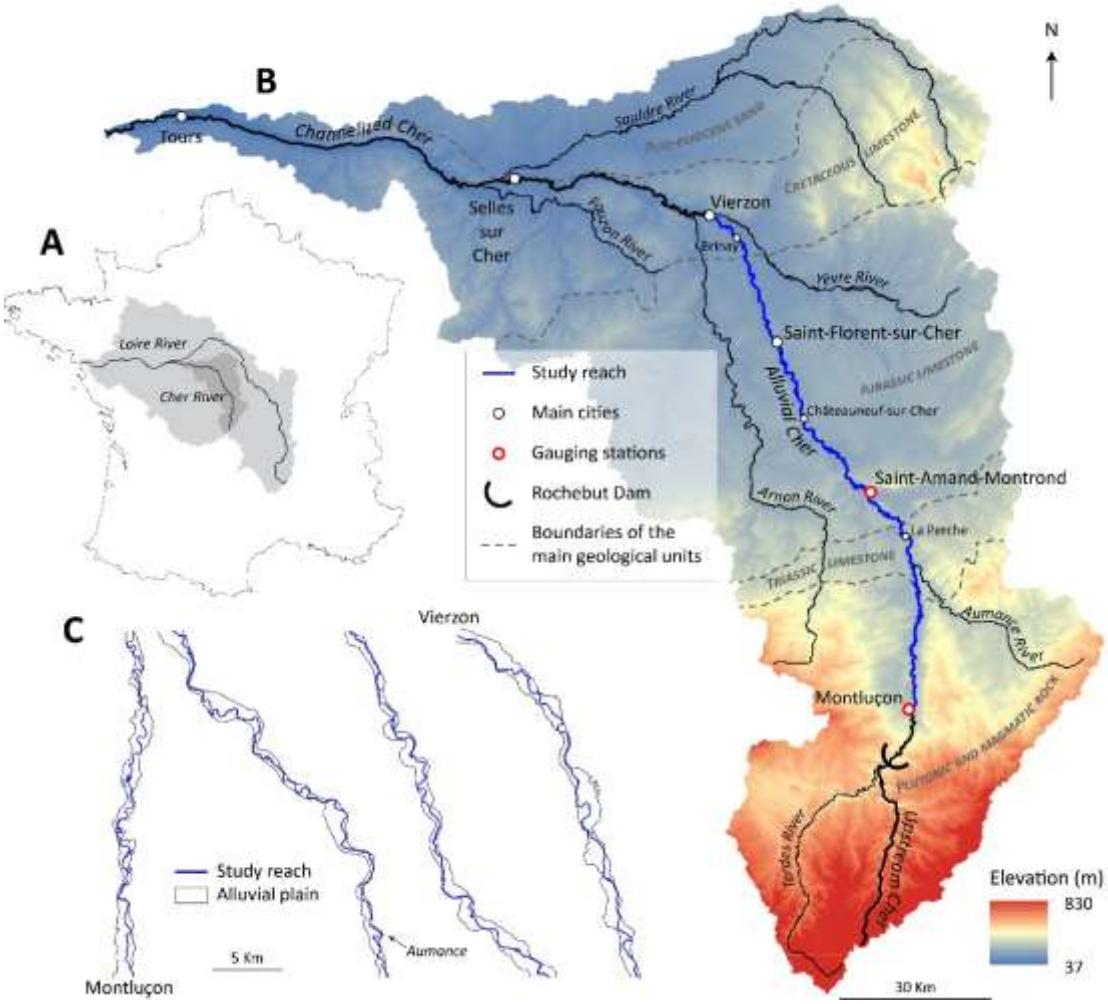

Figure 1 - Location of the study reach. A: The Cher River watershed within French territory. B: The study reach in the Cher River watershed. C: Diagram of the course of the Cher River and its alluvial plain.

3. Materials and methods

3.1 Reconstruction of bank retreat rates and length since the mid-20th century

The bank retreat rates and length of the river were reconstructed from aerial orthophotographs from the Institut Géographique National (IGN; National Geographic Institute) dated 1950s and 2016 using ArcGIS 10.6 (Table 1). For the 1950s, photographs

were dated 1954, 1959, and 1960, and they are subsequently referred to using the 1959 date alone, for which the majority of the active channel was digitized.

Quantification and characterization of bank retreat rates and length were based on the identification and digitization of the active channel at each date. Between the two successive dates, all areas occupied by perennial vegetation (islands and alluvial plain) at date t and active channel at date t+1 were considered eroded.

Table 1 – Date, scale, resolution (m) and rectification error (m) of aerial photographs used in reconstruction of bank retreat rates and length of the Cher River since the mid-20th century.

Date	Scale	Resolution	Rectification error
1954–1960	1/25000–1/27000	0.5	3.3
2016		0.2	3.2

Two main types of errors are inherent with the method used to generate the data (Gaeuman et al., 2003). The first corresponds to the rectification error (E1). The errors reported by the IGN for the 1959 and 2016 images are 2 m and 1 m, respectively. These errors are equal to the root mean squared error, which "summarizes the continuous deviations encountered over the ground surface (rather than at a few specific points)" (IGN, 2016). The second type of error corresponds to the active channel digitizing error (E2). It corresponds to the maximum uncertainty in locating the active channel boundary under overhanging forest. Obtained by iterative digitizing of its outline (Gurnell et al., 1994), it is equal to plus or minus 3 m for 1959 and 2016. Since these two errors are independent of each other, the total error,

equal to 3.3 m for 1959 and 3.2 m for 2016 (Table 1), was obtained by calculating the square root of the sum of the square of these errors (Taylor, 1997): $Totalerror = \sqrt{E1^2 + E2^2}$.

Once total error was determined, eroded areas were delineated. For each date, a buffer zone with a width equal to twice the value of the total error was created along each of the banks. The buffer zones of the active channel at two successive dates were then merged, denoting the spatial extent within which any change was considered unproven. Finally, any eroded polygon that was entirely within this merged buffer zone was excluded from the analysis. Conversely, when polygons exceeded the merged buffer zone, the change was considered proven and these polygons were retained. From these final eroded polygons the normalised retreat rates were computed at 50 m spaced cross-sections positioned perpendicular to the centerline of the active channel (ratio of retreat rate to the active channel width at the initial date expressed per year) (Roux et al., 2015). The normalised retreat rates were calculated for both banks combined and for concave banks alone. As there were no major changes in the river course, the longitudinal position of the cross-sections in 1959 and 2016 was determined from an origin located at the level of the Glacerie footbridge, in Montluçon. In addition, a certain number of river sections where gravel mining has led to an artificial widening of the bed were excluded from the analysis. Next, from the 50 m spaced cross-sections, the percentage of river length affected by lateral erosion was quantified every km. Finally, the longitudinal pattern of retreat rates and of the percentage of river length affected by lateral erosion were examined.

3.2 Evaluation of lateral constraints and space potentially available for channel shifting

Natural and anthropogenic structures, both present and from 1959, that directly constrain the potential lateral mobility of the river were characterized at each of the 50 m equidistant cross-

sections previously described. For natural constraints, digitized 1:50,000 scale geological maps from the Bureau de Recherches Géologiques et Minières (BRGM; French Geological Survey) were used (Debrand-Passard et al., 1977a, 1978; Lablanche, 1984, 1994; Manivit and Debrand-Passard, 1994; Obert et al., 1997; Turland et al., 1989a, 1989b). The maximum space available for channel shifting in absence of anthropogenic constraints was assigned to the location of the present and recent alluvium (fy/fz). Any cross-section with at least one bank abutting hillslope, alluvial or colluvial fan, or terrace was considered laterally constrained (Fryirs et al., 2016). Because of the relative spatial uncertainty of the boundaries between the alluvium and the hillslopes, fans or terraces, it was considered that abutting occurred when the distance between the river and the natural constraints is less than 50 m. The same approach was applied for concave banks only.

Four types of anthropogenic constraints were distinguished: bank protection, bridges, weirs, and gravel pits installed in the alluvial plain. If gravel pits could have been classified as a SEI, their presence also is a direct constraint on lateral mobility to the extent that lateral displacement of the river would be completely blocked for decades in the case of capture by a pit. For this reason, they were classified as a constraint to lateral mobility rather than as a SEI.

Bank protection works were identified and their positions surveyed by GPS in the field during the 2018 summer low flow. Bank protection works in 2018 located on sections of river not eroded between 1959 and 2016 were considered to be present in 1959. Bridges and weirs were identified and located from 1959 and 2016 aerial photographs and from the Référentiel des Obstacles à l'Ecoulement (Repository of obstacles to flow, ROE; https://www.sandre.eaufrance.fr/atlas/srv/fre/catalog.search#/map). On cross-sections located within 50 m of bridges and weirs, the river was considered constrained. Finally, gravel pits currently present in the alluvial plain were digitized by Cossalter (2011) from 2005 aerial photographs. This digitization was updated in the present work using 2016 aerial photographs.

Similarly, 1959 gravel pit locations were digitized from 1959 aerial photographs. Any cross-sections located within 50 m of a gravel pit were considered constrained.

Moreover, all current SEIs encountered in the floodplain, except those related to agricultural lands, also were integrated into the GIS analysis. Taking SEIs into consideration allows determination of the space potentially available for river shifting in the absence of lateral constraints, specifically in the case of restoration of lateral mobility. For each cross-section, the distance to the nearest SEI was measured, but SEIs were not prioritized. The raw data used were from the IGN Topo database. The GIS layers including important buildings, industrial buildings, cemeteries, sports grounds, water reservoirs, pylons, pipes of any kind, electricity lines, electrical substations, marshalling areas, stations, railroads, and the Berry Canal were used without modification. For the 'undifferentiated buildings' layer, polygons representing buildings judged non-essential were excluded (shelters, huts, etc.). Finally, the 'primary road' layer was kept unchanged, whereas the 'secondary road' layer was selected since roads and paths not accessing one of the objects listed above were excluded.

The extent of lateral constraints and/or SEIs in the floodplain was considered in two distinct but complementary ways. First, the percentage of river length affected by the different types of constraints and/or SEIs were quantified. We considered that a SEI is present along the river when it is located <50 m from the closest bank. The percentage of river length laterally constrained was calculated every km. In a second step, the space potentially available for channel shifting was measured at each 50 m spaced cross-section after taking into account the different types of constraints and/or SEIs. Here, all SEIs present in the floodplain were considered. The constrained length and the space potentially available for channel shifting were determined by considering both banks or just concave banks. Concave banks were the focus because this is where most of lateral erosion occurs. Thus, in a relatively short timescale (years to decades), and from the perspective of improving the ecological status of the river by

restoration of lateral erosion, the available floodplain space adjacent to this concave side is of direct interest for river managers. Finally, visual examination and Hubert's segmentation (Hubert et al., 1989; Hubert, 2000) were applied to determine the longitudinal pattern of (1) the percentage of river length affected by the different types of constraints and/or SEIs, and (2) the space potentially available for channel shifting.

3.3 Factors controlling lateral erosion

Bank retreat rates for the 1959–2016 period were related at different spatial scales to four of the main potential controlling factors reported in the literature: specific stream power (calculated for a discharge not exceeded 99% of the time) (e.g., Richard et al., 2005), curvature (e.g., Furbish, 1988; Sylvester et al., 2019), lateral constraints (Dépret et al., 2017), and the density of bars and alluvial riffles, used as an indicator of the coarse material available for bedload, the availability of a sufficiently large load of mobile coarse sediment being an indispensable condition for the self-maintenance of lateral mobility (e.g., Donovan et al., 2021). The assumed trends are an increase in retreat rates and in the occurrence of lateral erosion with an increase in each of these four factors.

First, the presence of any spatial correspondence between the longitudinal pattern of retreat rates or the percentage of river length affected by lateral erosion on one hand, and the longitudinal pattern of specific stream power, curvature, lateral constraints, and the density of bars and alluvial riffles on the other hand was evaluated.

Second, at the scale of unconstrained cross-sections, the extent to which specific stream power and curvature at the initial date differed between cross-sections with erosion and cross-sections without erosion was examined. Then, for cross-sections subjected to erosion only, correlations between retreat rates and specific stream power or local curvature

were calculated. In a second step, a Chi-square test was performed to determine the influence of lateral constraints present in 1959 on the manifestation of lateral erosion.

Specific stream power was obtained using the formula: $\rho_w g Q S / w$, where ρ_w is the density of water (1000 kg m^{-3}), g is the gravitational acceleration (9.81 m s^{-2}), Q is the discharge (m^3 s^{-1}), S is the bed slope (m m^{-1}), and w is the active channel width (m). The specific stream power was determined for each 50 m equidistant cross-section using the low-water line slope from the laser imaging detection and ranging digital elevation model (LiDAR DEM) data of the Cher Valley (2011) and the 1959 active channel width. A discharge with the same non-exceedance frequency (not exceeded 99% of the time) was used upstream and downstream of the confluence with the Aumance River in order to make the two sub-reaches comparable. It was equivalent to 90 m^3 s^{-1} for the upstream sub-reach (Montluçon reference gauging station) and 190 m^3 s^{-1} for the downstream sub-reach (Saint-Amand-Montrond reference gauging station), values similar to the bankfull discharge on each of the sub-reaches (85 m^3 s^{-1} upstream and 178–245 m^3 s^{-1} downstream) (Dépret, 2014).

Curvature was calculated locally at each cross-section. This corresponds to the angle (in radians per m) between the centerline segment connecting the upstream cross-section and the cross-section in question on the one hand, and the centerline segment connecting the cross-section in question and the downstream cross-section on the other. The curvature was then normalized against the width of the active channel to make comparable the sub-reaches upstream and downstream of the Aumance junction (rad m^{-1} m^{-1}). Lateral constraints in 1959 were identified as described in Section 3.2.

Bars, alluvial riffles, and rocky riffles were identified and their positions surveyed by global positioning system (GPS) in the field during the 2018 summer low flow. During this same campaign, the presence of bedrock in the bed (other than in the form of rocky riffles) also was systematically surveyed. Thereby the length of the sections along which bedrock is

outcropping and the distance between the sections in question were acquired. However, these sections are somewhat heterogeneous, since they include both sections of the river along which the alluvium has been completely evacuated and sections where the bedrock outcrops are laterally and/or longitudinally more or less discontinuous. Due to the different widths of the river upstream and downstream of the confluence with the Aumance, the distance between two successive units or the length of the bedrock sections was normalized against the width of the river.

3.5 Preservation and restoration of lateral mobility

Herein, identification of river sections for which measures to preserve or to restore lateral mobility could be undertaken is done. The main objective was to propose a synthetic image of each of these sections that could be used by managers as a decision-making tool. The sections likely to be most suitable for restoration of lateral mobility are those equipped with bank protection, the only type of constraint that can be removed. The approach utilized included three stages. First, sections presenting *a priori* a minor interest in terms of preservation or restoration of lateral mobility were excluded (see paragraph below for detailed explanation). Next, based on the remaining sections to be preserved, the intensity of retreat rates can be explained from the values for tested controlling factors in 1959 using logistic regression models. Finally, the generated models were applied using the values of controlling factors in 2016 to predict retreat rates for the sections to be preserved or restored. The various criteria taken into account in this analysis were incorporated at an elementary level at the scale of cross-sections spaced 50 m apart. The values finally retained at the scale of the considered sections correspond to the mean or median of values informing the cross-sections encountered on each section.

For preservation, sections with at least one of the following criteria were excluded: maximum retreat rate in concave bank <0.017 m m^{-1} y^{-1}, length <100 m, space potentially available for channel shifting in concave bank ≤100 m, specific power in 2016 for a discharge not exceeded 99% of the time ≤13 W m^{-2}. The use of a threshold value for retreat rates allows the exclusion of sections without erosion between 1959 and 2016. This criterion appears to be essential because a section without erosion in recent decades is unlikely to present lateral erosive activity in the future. The chosen threshold of 0.017 m m^{-1} $year^{-1}$ corresponds to the value for which the performance of the logistic regression model used to explain and predict retreat rates at the section scale was optimized. In addition, this threshold allows the focus to be exclusively on the most historically active reaches. The section length and the space potentially available for channel shifting criteria were set so that the manifestation of lateral erosion could ensure a sustained and long-lasting injection of coarse sediments into the active channel. The selected length of 100 m corresponds to the median of the length of the eroded sections between 1959 and 2016. The minimum envelope of 100 m retained for the space potentially available for channel shifting makes it possible to ensure maintenance of erosion over several decades without having to intervene to protect SEIs currently relatively far from the bed. This value of 100 m corresponds to the most important bank retreat measured between 1959 and 2016 along the study reach. The space potentially available for channel shifting retained is equal to the median of the values on the concave side at the level of the cross-sections present at each river section. Finally, the value of 13 W m^{-2} was chosen based on monitoring of eroded banks between 2009 and 2013 at two sites located upstream and downstream (kilometric point (kp) 26.45-37.1 and kp 61.4-69.9) of the confluence with the Aumance (Dépret, 2014). The value of 13 W m^{-2} corresponds to the lowest specific stream power for a discharge not exceeded 99% of the time at these different monitoring sites.

Once sections meeting at least one of these criteria were excluded, a logistic regression model adapted to beta-type distributions (values taken by individuals of the dependent variable between 0 and 1) was applied. For this, the GAMLSS package of R (Rigby and Stasinopoulos, 2005) was used. Two regression models were constructed to explain the mean and maximum concave bank retreat rates between 1959 and 2016 along the sections to be preserved. The two independent variables ultimately selected were the maximum specific power in 1959 for a discharge not exceeded 99% of the time and the mean local curvature in 1959. The generated models then were applied to predict retreat rates from the maximum specific stream power in 2016 and the mean local curvature in 2016.

For restoration of lateral mobility, the considered sections include river sections with concave bank protection extending from contiguous upstream and/or downstream river sections without bank protection. As a result, there is a partial overlap between some sections to be preserved and some sections that may be restored. The same exclusion criteria as presented for the sections to be preserved were applied, with the exception of the criterion relating to erosion. Two other criteria also were added: a very small amount of bank protection (proportion of river length ≤20% of the length of the sections or a length of bank protection equal to 50 m, which corresponds to the minimum length of the protection since the latter were informed on the scale of the cross-sections), and the presence of SEIs immediately downstream of the sections equipped with bank protection. Logistic regression models then were used to predict the mean and maximum erosion rates along each of the sections identified as suitable for restoration.

4. Results

4.1 Characteristics of planimetric erosion between 1959 and 2016

Mean and median bank retreat reached 0.0107 and 0.0067 m m^{-1} $year^{-1}$, respectively, when both banks were considered, and 0.012 and 0.0075 m m^{-1} $year^{-1}$ when only concave banks were taken into account (Figure 2). The retreat rates showed a main break at kp 70.15 when both banks were considered and kp 69.8 when only concave banks were taken into account (Figure 3A). Downstream of these points, retreat rates were on average 4.1 and 2.7 times lower for both banks and concave banks, respectively. A less sharp break also occurred at kp 44.6. The reach upstream of this point had the highest retreat rates.

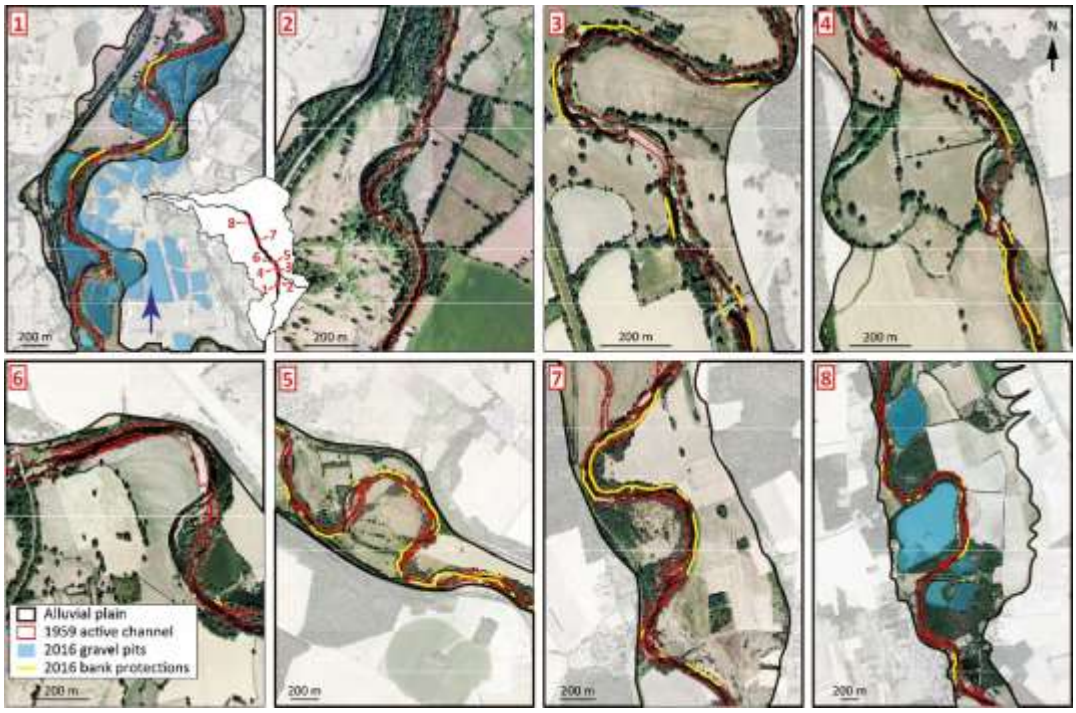

Figure 2 – Examples of active channel displacements from 1959 to 2016, and some of the main current constraints of bed mobility. The reaches are numbered in ascending order from upstream to downstream (with their location indicated between subfigures of reaches 1 and 2).

Between 1959 and 2016, bank erosion occurred on at least one bank along 380 discrete sections (comprising 40% of the river length). The 380 eroded sections have a mean-

median length of 130–100 m. The longitudinal pattern shows a main break at kp 71, very close to the main break identified for the retreat rates (Figure 3B). Downstream of this point, the percentage of eroded river length per km is 1.6–1.9 (mean-median) and 2.3–2.9 times lower than upstream, when considering all banks or only concave banks, respectively.

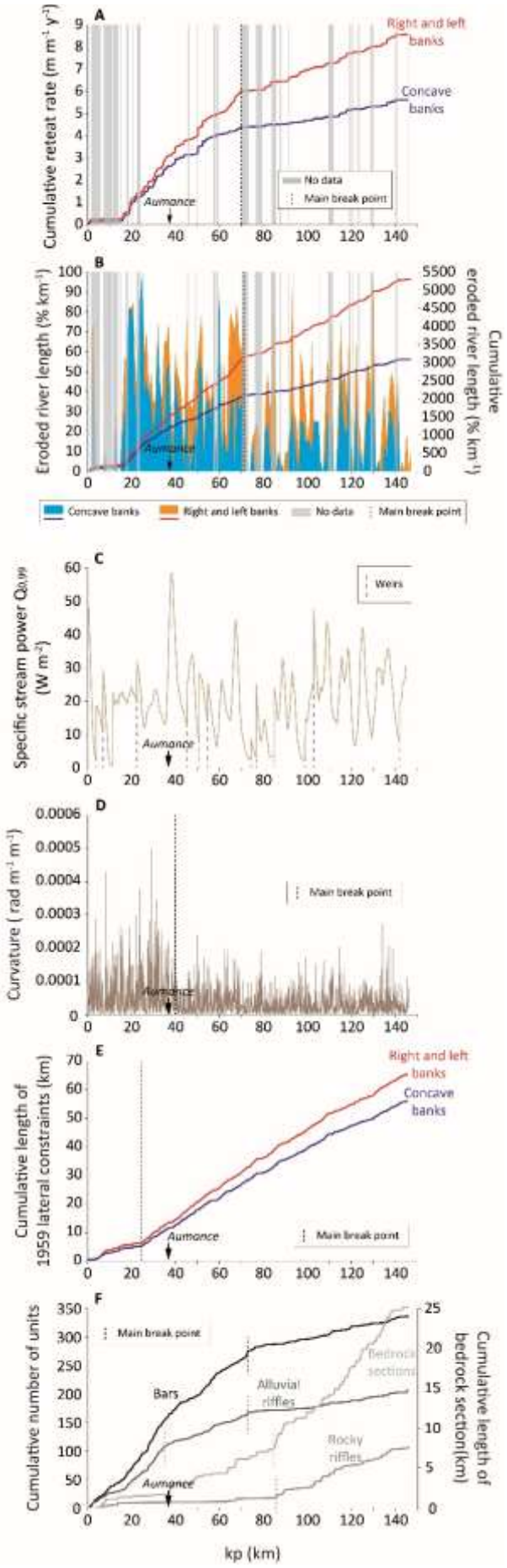
A
Cumulative reteat rate (m m⁻¹ y⁻¹)
Right and left banks
Concave banks
No data
Main break point
Aumance
B
Eroded river length (% km⁻¹)
Cumulative eroded river length (% km⁻¹)
Concave banks
Right and left banks
No data
Main break point
C
Specific stream power Q0.99 (W m⁻²)
Weirs
D
Curvature (rad m⁻¹ m⁻¹)
Main break point
E
Cumulative length of 1959 lateral constraints (km)
Right and left banks
Concave banks
Main break point
F
Cumulative number of units
Cumulative length of bedrock section(km)
Main break point
Bars
Alluvial riffles
Rocky riffles
Bedrock sections
kp (km)

Figure 3 – Longitudinal pattern of (A) planimetric retreat rates between 1959 and 2016, (B) percentage of eroded river length and cumulative percentage of eroded river length between 1959 and 2016, (C) 2016 specific stream power for a discharge not exceeded 99% of the time, (D) 2016 local curvature, (E) cumulative length of lateral constraints in 1959 and (F) bars, alluvial riffles and rocky riffles in 2018.

4.2 Bed confinement and space potentially available for channel shifting

In this section, the extent to which engineering works, the legacy of human activities, and SEIs identified in the valley bottom contribute to the current lateral confinement of the Cher is examined (see examples in Figure 2). The initial focus is on the river length affected by these constraints, then the focus shifts to the space potentially available for channel shifting.

4.2.1 Description and quantification of laterally constrained river length

The Cher River is a partially confined river based on criteria established by Fryirs et al. (2016); 19.2% of its length is within 50 m of a terrace, alluvial or colluvial fan, or hillslope (Figure 4A). Its mobility is, therefore, naturally constrained in many locations. If we add to these natural constraints all the anthropogenic physical obstacles, the channel cannot shift over 56% of its length (Figure 4A and Figure 5). Engineering works or legacy of human activities are, therefore, responsible for a 2.9-fold increase in the length of the river along which lateral erosion is now impeded. If we add to these 'primary' anthropogenic constraints all of the SEIs identified in the alluvial plain <50 m from the banks, the length laterally constrained reaches 63% (Figure 4A). Bank protection accounts for the largest proportion of the constraints on lateral mobility, since they occupy 35.1% of the river length on either bank (Figure 4A), followed by gravel pits at 10.9%. If only concave banks are considered, the length along which the river cannot move laterally rises to 46.9% (compared with 15.6% for

natural constraints alone) after all constraints are taken into account, and to 53.1% when SEIs are added (Figure 4A). Bank protection occupies 29% of the total length, and gravel pits account for another 6.1%.

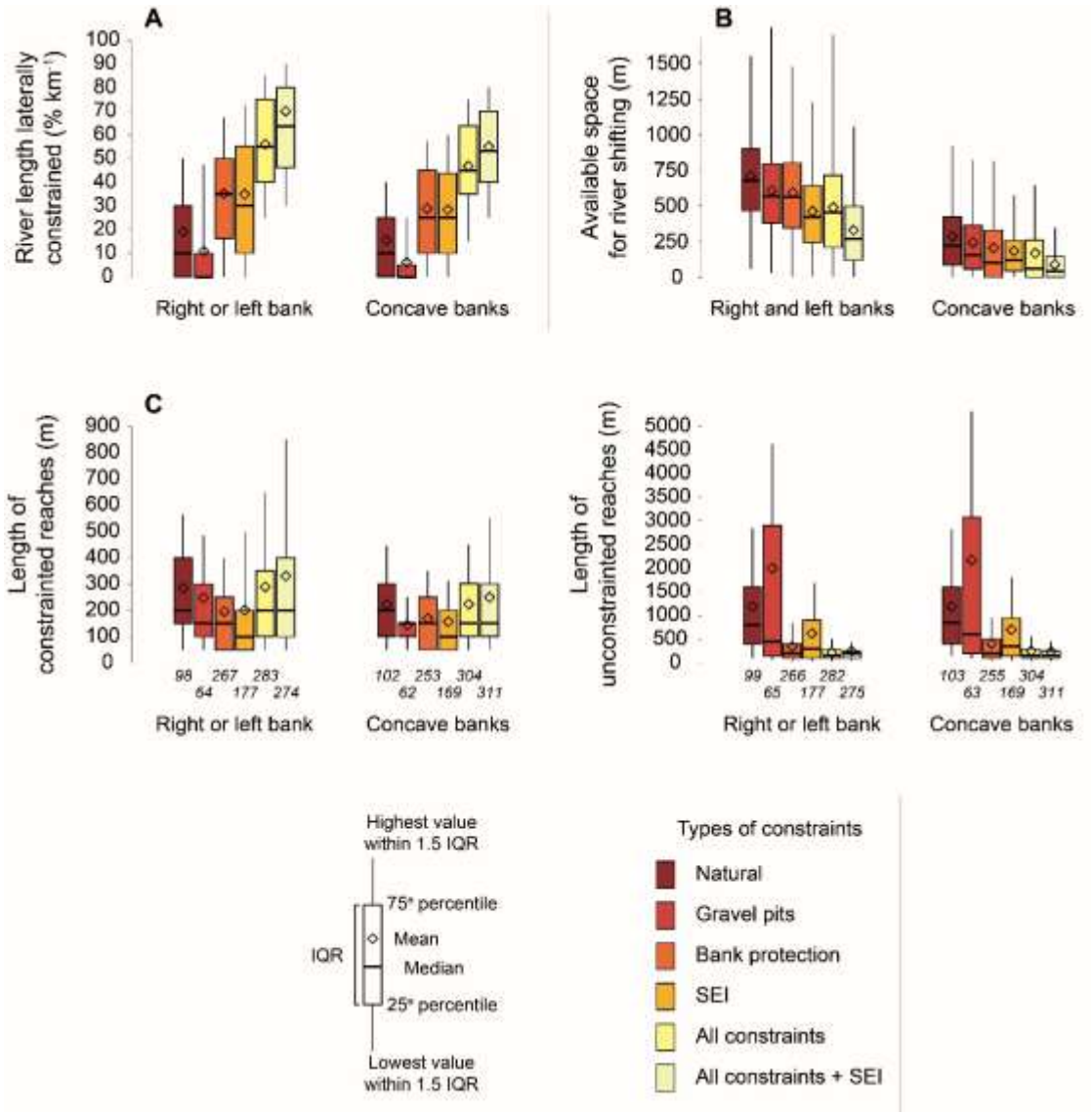

Figure 4 – Boxplots of the current percentage of river length laterally constrained as a function of types of lateral constraints (A), current maximum space available for channel shifting as a function of types of lateral constraints (B), and current length of constrained and unconstrained reaches as a function of types of lateral constraints (C).

Despite important local variability, the longitudinal pattern of the different types of constraints tends to be stable (Figure 5). For gravel pits, four main sections are nevertheless visually identifiable (Figure 5).However, Hubert's segmentation (Hubert et al., 1989; Hubert, 2000) indicates only the upstream section (Figure 5). Although bank protection is present along the entire length of the river, Hubert's segmentation highlights a long central reach that is more densely equipped, extending from kp 21 to 76 (Figure 5). The reduced presence of bank protection in the first 21 km of the study reach could be because a significant proportion of the river length of this section had its course and banks artificially modified during gravel mining. With the exception of two short peaks at the upstream and downstream ends of the study reach, SEIs are distributed in a relatively regular and stable manner (Figure 5). The constraints or constraints plus SEIs show a similar pattern, with maximum values for the first 16 km, a short section with very few constraints and/or SEIs (kp 17–20), then stability for the rest of the length (Figure 5).

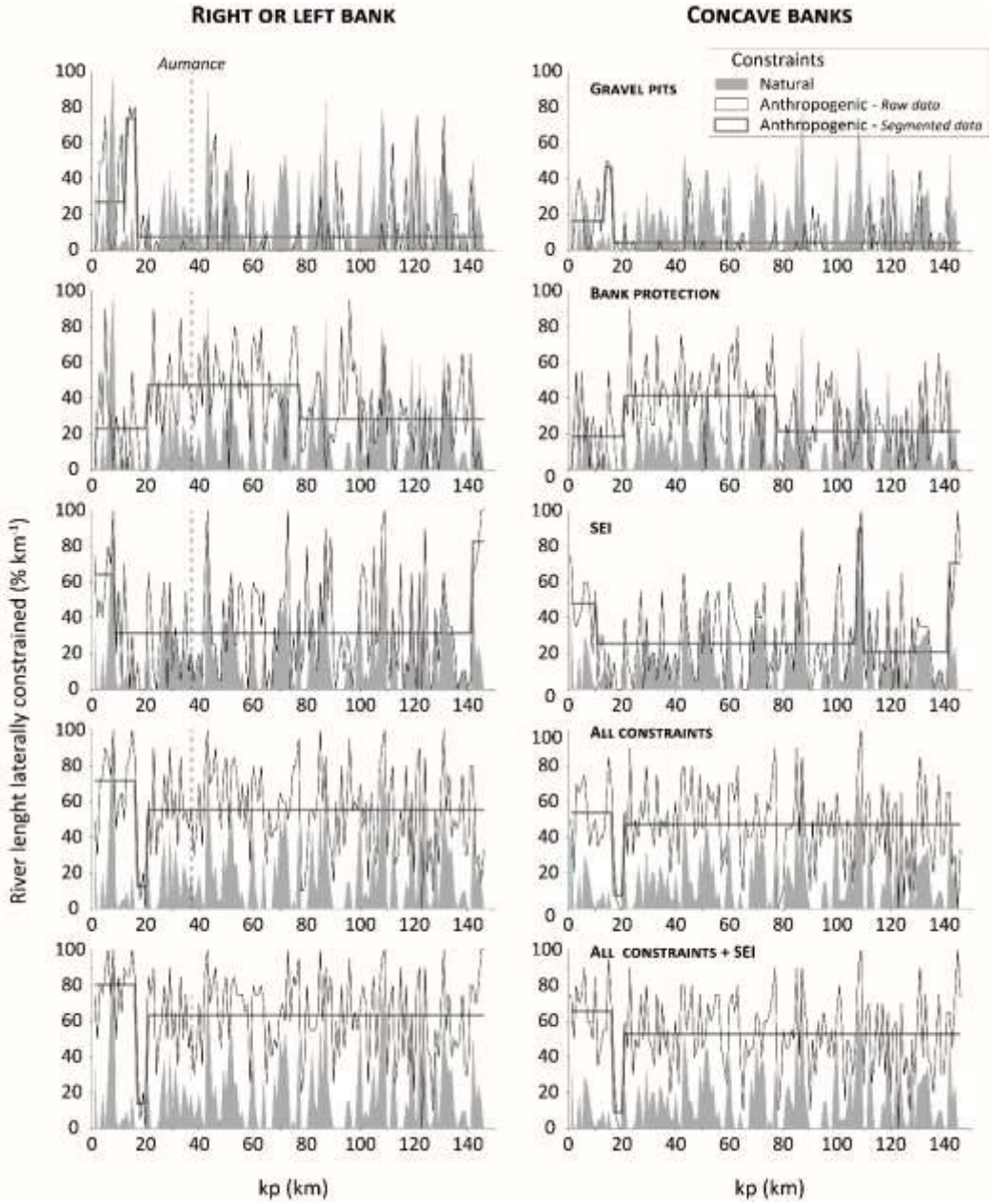

Figure 5 – Current longitudinal pattern of the percentage of river length laterally constrained as a function of constraint types. Segmented data were obtained by applying the Hubert method (Hubert et al., 1989; Hubert, 2000).

This foregoing reduction in river length along which bed migration is prevented is automatically accompanied by an increase in the longitudinal fragmentation of the bed (Figure 4C). The number of laterally unconstrained reaches is 99 when only natural constraints are considered, whereas it is 282 when all constraints are included. As a result, the

distance between two consecutive sections abutting against constraints decreases sharply; 1190–800 m (mean-median) with only natural constraints considered, compared with 227–150 m after incorporating anthropogenic constraints and 201–100 when SEIs are added (Figure 4C). The length of laterally constrained sections varied much less; 285–200 m with natural constraints, 290–200 m with all constraints and 330–200 m after incorporating all SEIs (Figure 4C).

For concave banks alone, the number of sections without natural lateral constraints is 103 and 304 once anthropogenic constraints are incorporated (Figure 4C). The distance between two consecutive constrained reaches is 1195–850 m with natural constraints alone, 255–150 m once all constraints are incorporated, and 220–150 m with additional consideration of SEIs (Figure 4C). The length of constrained reaches is 220–200 m with natural constraints, 224–150 m with all constraints, and 249–150 m after addition of SEIs (Figure 4C).

4.2.2 Space potentially available for channel shifting

The alluvial plain width (i.e,. the maximum space potentially available for channel shifting) is 707–678 m (mean-median; Figure 4B), and slightly lower upstream of the confluence with the Aumance River. However, the confinement index (ratio between the width of the alluvial plain and the width of the active channel) is higher in this upstream reach (18.3–17.6 vs. 14.3–13.7).

If all anthropogenic physical obstacles (bank protection, bridges, weirs, gravel pits) are added to the natural lateral constraints, the space potentially available for channel shifting decreases to 489–455 m (Figure 4B). This is equivalent to a reduction of 31–33%. After taking into account both constraints and SEIs, the space potentially available for channel shifting is only 330–267 m (i.e., a reduction of 53–61%; Figure 4B).

If we focus only on concave banks, the contraction of the maximum space potentially available for channel shifting is even larger. The maximum envelope shrinks from 281–221 m (mean-median) to 168–61 m when anthropogenic constraints are taken into account (i.e., a reduction of 41–73%; Figure 4B). After incorporating SEIs, the maximum space potentially available for channel shifting is then only 111–43 m, equivalent to a reduction of 61–81% (Figure 4B).

Regardless of the type of anthropogenic constraints considered, the longitudinal pattern of space potentially available for channel shifting remains relatively stable despite significant local variations (Figure 6). Moreover, the integration of anthropogenic constraints tends to homogenize this longitudinal variability.

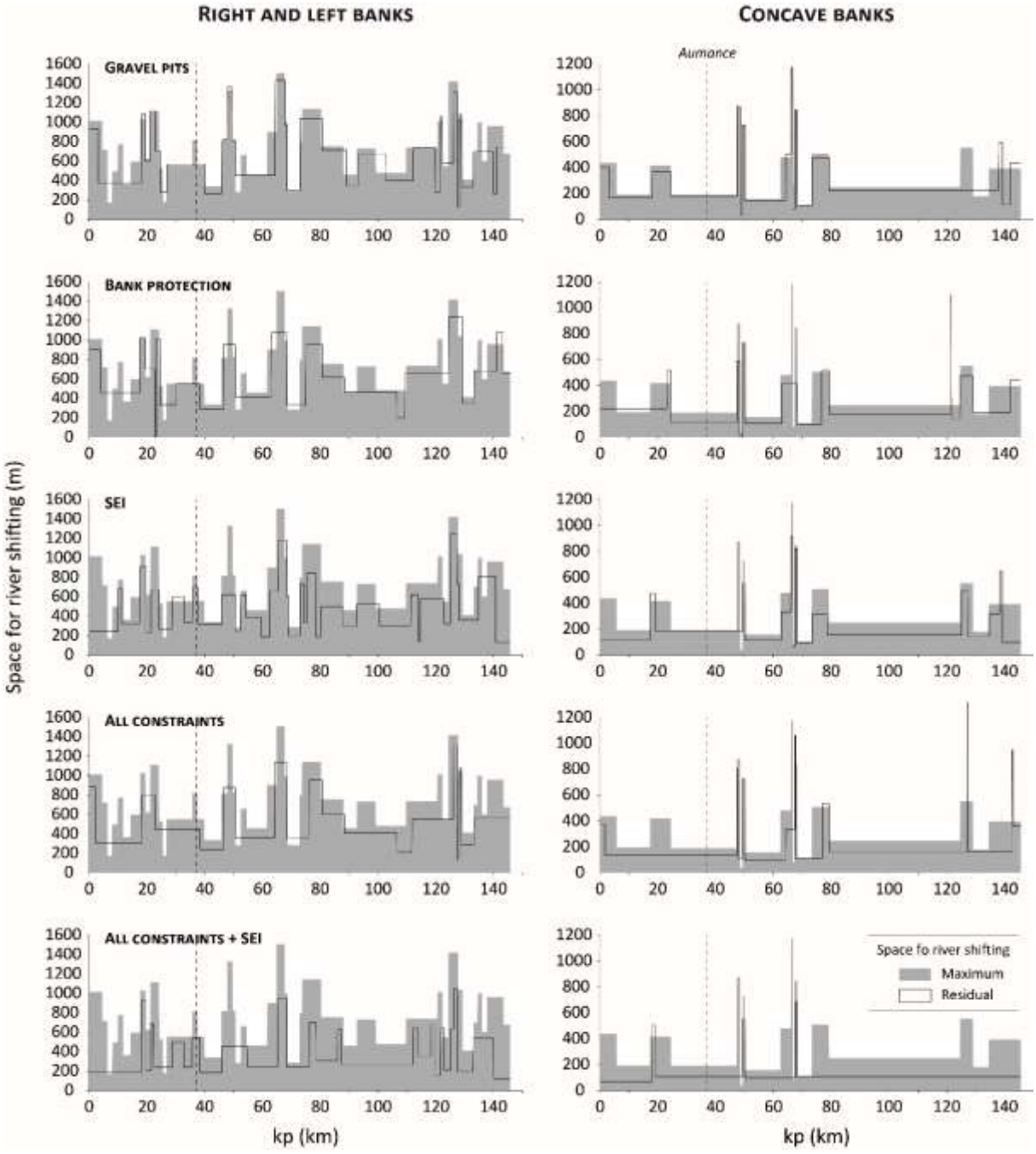

Figure 6 – Current longitudinal pattern of the space potentially available for channel shifting as a function of the types of constraints. For the sake of readability, data have been 'smoothed' using Hubert's segmentation method (Hubert et al., 1989; Hubert, 2000).

4.3 Factors controlling the intensity and location of lateral erosion

The longitudinal pattern of the specific stream power shows local variations that can be high, but no overall tendency to decrease or increase (Mann-Kendall test, p >0.1; Figure

525 3C). One of the main causes of these variations is the existence of many weirs, which results
526 in a strong reduction of specific stream power in their reservoirs, and an even more marked
527 increase immediately downstream. The decrease in erosive activity observed from about kp
528 70 during the 1959–2016 period (Figure 3A, B) is, therefore, not the result of an associated
529 decrease in specific stream power. Regarding curvature, a main break is visible at kp 39.6,
530 just downstream of the junction with the Aumance River, with a two-fold diminution of
531 curvature values (Mann-Whitney test, p <0.05; Figure 3D). This could explain the second
532 highest decrease in retreat rates, reported from kp 44.6. For lateral constraints in 1959, a
533 twofold decrease is observed downstream of the main break, located at kp 24.45 (Figure 3E).
534 On both sides of this point, lateral constraints are quite regularly distributed. There is
535 nevertheless an important uncertainty regarding the density of lateral constraints in 1959
536 along this upstream reach; most of this reach has been artificially redesigned due to gravel
537 mining in the 1970's, and it is not known to what extent bank protection was present before.
538 The reduced presence of bank protection in the first 24 km of the study reach could thereby
539 result from a significant proportion of the river length in this section having its course and
540 banks artificially modified during gravel mining. In any case, there is no spatial
541 correspondence between the longitudinal patterns of erosive activity during the 1959–2016
542 period and of lateral constraints in 1959 (or even in 2016, see Figure 5).
543 The 2018 longitudinal pattern of bars, alluvial riffles, rocky riffles, and bedrock sections
544 indicates two main reaches (Figure 3F); in the upstream reach, bars and alluvial riffles are
545 frequent, while rocky riffles and bedrock sections are rare, and this trend is reversed in the
546 downstream reach. For bars and alluvial riffles, the main break, located at kp 72.8 and 72.7,
547 respectively, is slightly downstream of the break in erosive activity (kp 70). The mean spacing
548 between bars and between alluvial riffles, therefore, increases from 6.3 to 23.8 bankfull
549 widths for the former and from 10.6 to 36.8 bankfull widths for the latter (Mann-Whitney test,

550 p <0.05; Figure 3F). In addition, for alluvial riffles, the upstream reach can be divided into
551 two sub-reaches with a limit located at kp 34.9, with a mean spacing of 8.9 bankfull widths
552 upstream and 13.5 bankfull widths downstream (Mann-Whitney test, p <0.05). For rocky
553 riffles, the break is located at kp 85.5 (Figure 3F). The mean spacing between rocky riffles
554 decreases significantly from upstream to downstream, from 110 to 13.8 bankfull widths
555 (Mann-Whitney test, p <0.05). For bedrock sections, the limit is located at kp 84.5 (Figure
556 3F). Upstream, the mean length of bedrock sections and the distance between two consecutive
557 sections are 5.6 and 62 bankfull widths, respectively. Downstream, they are 9.6 and 23.4
558 bankfull widths.

559 Examined at the cross-section scale, the influence of specific stream power on the
560 manifestation of erosion appears to be absent; in the absence of lateral constraints and when
561 both banks are considered, the mean specific stream power is 22.7 W m^{-2} and 22.3 W m^{-2} for
562 cross-sections with and without erosion, respectively (Mann-Whitney test, p = 0.83; Figure
563 7A). Focusing on concavities alone, the mean stream power is 22.8 W m^{-2} and 21.7 W m^{-2}
564 (Mann-Whitney test, p = 0.1; Figure 7A). Conversely, local curvature probably exerts a
565 significant influence since they are 1.8 times higher on cross-sections with erosion when both
566 banks are considered and 1.6 times higher when considering concave banks alone (Mann-
567 Whitney test, p <0.000001; Figure 7A). Finally, for cross-sections subjected to erosion, no
568 correlation was detected between the normalized retreat rate on the one hand, and the specific
569 stream power or the local curvature on the other hand (Figure 7B).
570

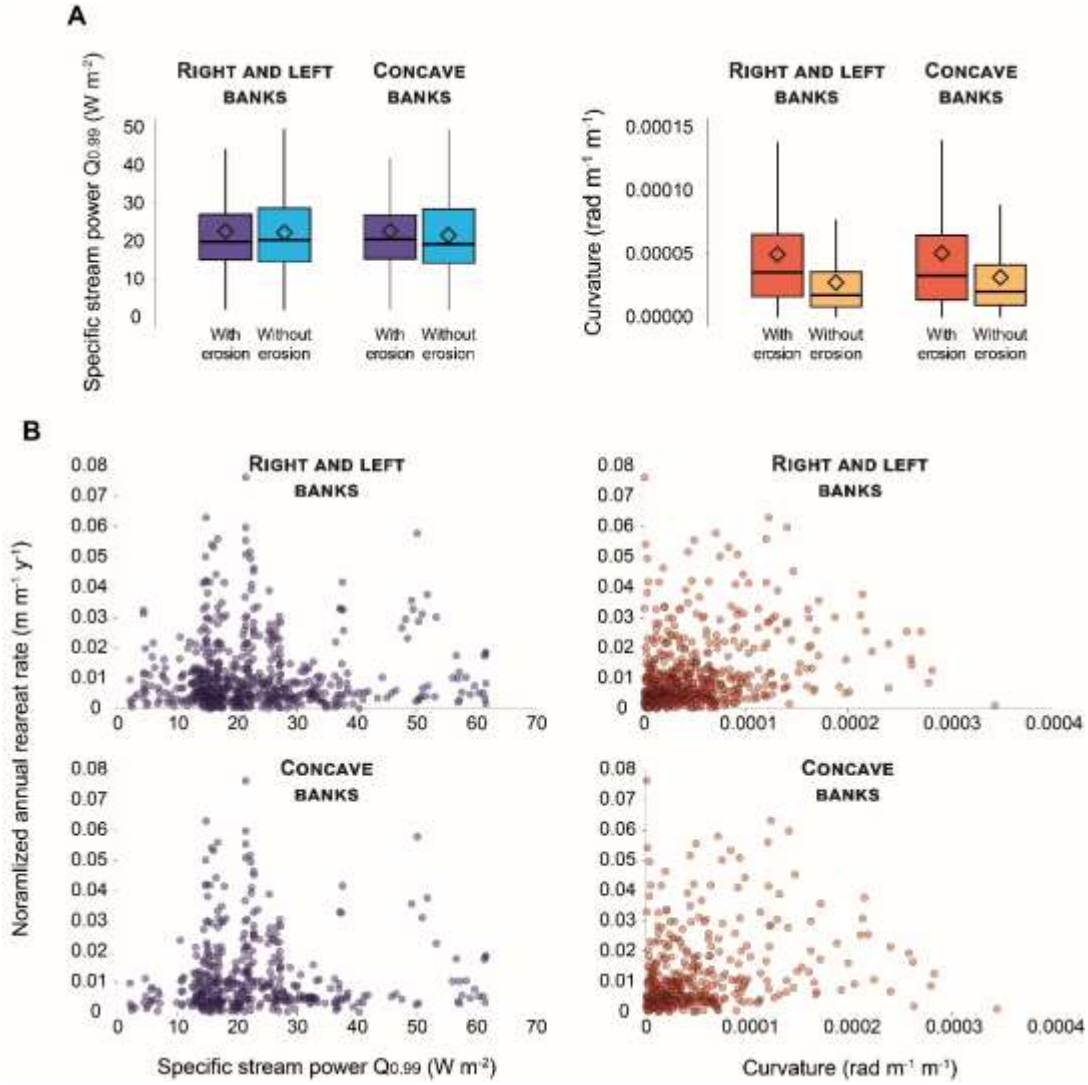

Figure 7 – Comparison of specific stream power for a discharge not exceeded 99% of the time and of curvature between eroded and non-eroded unconstrained cross-sections (A). Relation between the normalized annual retreat rate and the specific stream power for a discharge not exceeded 99% of the time and the curvature of eroded cross-sections (B).

Lateral constraints play a major role in the expression of lateral erosion. Indeed, there was a statistically significant difference in erosion between constrained and unconstrained banks (Chi-square test, p <0.00001; Table 2); 67% of cross-sections with erosion are located where constraints are absent, while 60% of cross-sections without erosion are located where constraints are present. Furthermore, 72% of cross-sections subjected to lateral constraints

escape erosion, and the proportion drops to 46% for cross-sections not influenced by lateral constraints. If we consider only concave banks, the role of constraints appears even more significant since 83% of eroded cross-sections are located where constraints are absent and 90% of cross-sections subjected to lateral constraints escape erosion.

Table 2 – Presence-absence of lateral constraints and lateral erosion on cross-sections spaced 50 m apart. Statistical differences were determined using the Chi-square test.

	Lateral constraints	No lateral constraints	*p*-value
Right or left bank			
Erosion	260	524	<0,00001
No erosion	656	442	
Concave banks			
Erosion	79	717	<0,00001
No erosion	703	383	

4.5 Preservation and restoration of lateral mobility: priority elements

The developed logistic regression models provide a relatively good explanation of the concave bank retreat rates between 1959 and 2016 on sections prioritized for preservation of lateral mobility (Table 3 ; Figure 8). Just over 50% of the variance in retreat rates is explained by the maximum specific stream power and the mean local curvature along the sections, with both variables playing a significant role (Table 3). The equations for the prediction of the maximum (Eq.1) and the mean (Eq.2) retreat rates are:

598 Logit (Maximum annual normalized retreat rates) =

599 $-4.107 + 0.02562 \times$ maximum specific stream power $+ 3728 \times$ mean curvature

600 (Eq.1)

601

602 Logit (Mean annual normalized retreat rates) =

603 $-5.279 + 0.03772 \times$ maximum specific stream power $+ 4784 \times$ mean curvature

604 (Eq.2)

605

606

607 Table 3 – Logistic (logit) regression coefficients explaining the maximum annual normalized
608 retreat rates (m m^{-1} $year^{-1}$) and the mean annual normalized retreat rates (m m^{-1} $year^{-1}$) as a
609 function of maximum specific stream power (W m^{-2}) and mean curvature (rad m^{-1} m^{-1}) (R^2 =
610 Coefficient of determination).

	Coefficient	Standard error	t	*p*-value	Pseudo-R^2 (Cox and Snell)
Logit (Maximum annual normalized retreat rates)					
Interception	-4.107	0.1678	-24.48	***	
1959 maximum specific stream power	0.02564	0.005298	4.84	***	0.53
1959 mean curvature	3728	1602	2.33	*	
Logit (Mean annual normalized retreat rates)					
Interception	-5.279	0.2499	-21.13	***	
1959 maximum specific stream power	0.03772	0.007577	4.98	***	0.52

1959 mean curvature	4784	2336	2.05	.

611

612 *p*-values *** = 0, * = 0.01, . = 0.05.

613

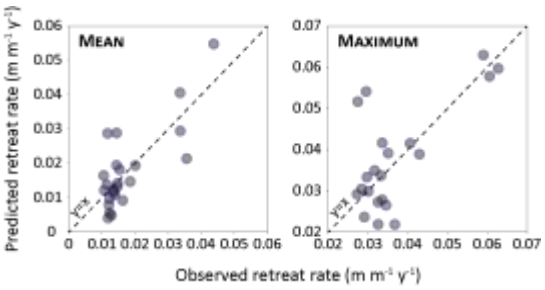

614

615 Figure 8 – Relations between predicted and observed retreat rates for concave banks between
616 1959 and 2016 along unconstrained sections identified as a priority for preservation of lateral
617 mobility.

618

619 If the preservation and restoration sections have similar predicted retreat rate values,
620 they show a clear difference in the length and the space available for river shifting, with
621 preservation sections significantly having shorter length but larger space for river shifting
622 (Figure 9).

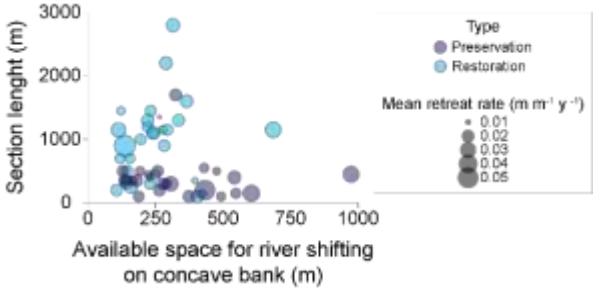

623

624 Figure 9– Length versus available space for river shifting on the concave side, and predicted
625 mean concave retreat rates along sections identified as a priority for preservation or
626 restoration of lateral mobility.

627

Twenty-four sections of the river are of particular interest in terms of preserving lateral mobility (Figure 10). They extend over a total length of 9.3 km (6.3% of the length of the study reach). Most are located upstream, between kp 15.9 and 69 (20 sections out of 24 and 84.3% of the total length of the sections), consistent with the decrease in erosive activity identified downstream of kp 70 (Figure 10).

After elimination of sections of less interest from the point of view of restoring river lateral dynamics, 30 sections remain from the initial 112, extending over 69.2 km, 45.9% of which have bank protection (Figure 10). These 30 sections represent a total length of 28.6 km, or 19.7% of the length of the study reach, and bank protection occupies 11.3 km, namely 39.3% of the total length of the 30 sections. Compared with the conservation sections, the restoration sections are more evenly distributed along the study area (Figure 10), but there is also a high concentration of these restoration sections upstream; 12 of the 30 restoration sections are located between kp 26.6 and 48.6, over 20 km (15.1% of the study reach length). Moreover, these 12 sections represent 76.9% of the total length of the restoration sections.

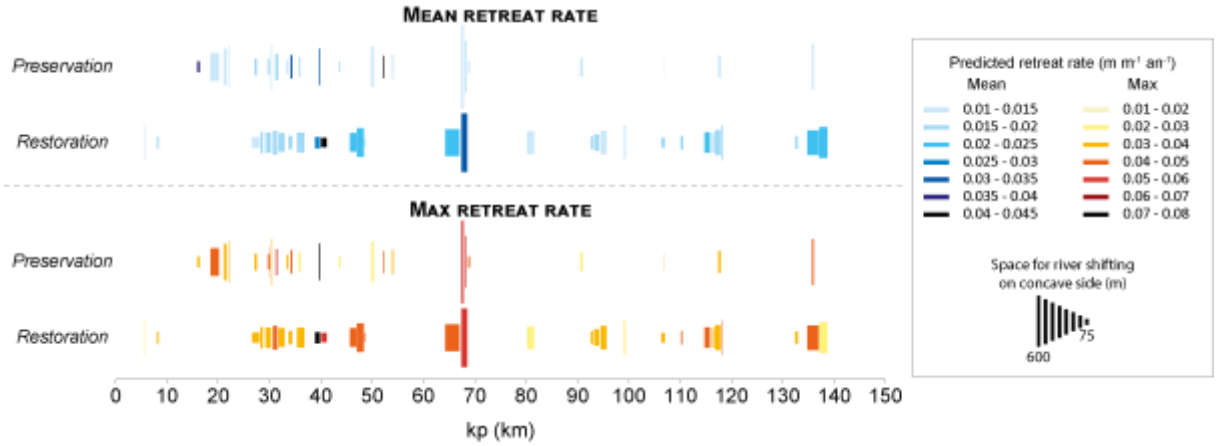

Figure 10 – Localization and characteristics of sections identified as a priority for preservation or restoration of lateral mobility. The predicted retreat rates were computed from equations in Table 3, with 2016 values for specific stream power and curvature.

5. Discussion

5.1 Performance of logistic regression models

The logistic regression models developed for reaches of high interest for preserving or restoring lateral mobility explain slightly more than 50% of the variance in the maximum or mean lateral erosion between 1959 and 2016 (Pseudo-R^2 in Table 3). Other controlling factors not considered here (maximum specific power in 1959 and mean curvature in 1959) should, therefore, be considered. They were not included in the model due to insufficient data. The first such controlling factor is heterogeneity of bank strength, driven by bank height and morphology, the type of vegetation covering banks (e.g. Ielpi and Lapôtre, 2020; Horton et al., 2017; Micheli and Kirchner, 2002; Micheli et al, 2004; Piégay et al., 2003), and the spatial heterogeneity of the alluvial infill material (e.g., Bogoni et al., 2017; Constantine et al., 2009; Fisk, 1944, 1947; Güneralp and Rhoads, 2011; Motta et al., 2012). The second controlling factor is the spatial variability in the bedload supply, a major driver of lateral mobility in meandering streams (Ahmed et al., 2019; Constantine et al., 2014; Donovan et al., 2021; Dunne et al., 2010; Rollet and Piégay, 2013). The third controlling factor is the bed material D_{50}, theoretically conversely correlated with bank retreat (Bledsoe and Watson, 2001; Richard et al., 2005). The fourth controlling factor is the effect of lateral constraints on contiguous river sections devoid of such constraints, where bank erosion can be inhibited/prevented or, conversely, promoted. The fifth controlling factor is gravel mining in the riverbed that can increase lateral erosion by destabilizing banks (Schumm et al., 1984; Simon, 1989; Simon and Rinaldi, 2006; Watson et al., 2002), and the presence of undetected blocks of former bank protection located in the riverbed that can conversely slow bank retreat (Dépret et al., 2017).

Compared with similar analyses that attempted to explain and/or predict lateral erosion of meandering rivers computed from sequential aerial photographs through statistical

modelling at decadal or multi-decacal scales, the percentage of explained variance in the current study can be considered more satisfactory. For example, in four reaches of the Rio Grande River, U.S., Richard et al. (2005) obtained coefficients of determination (R^2) between 0.43 and 0.93 explaining absolute migration rates with parameters representing flow energy used alone (either the mobility index of Bledsoe and Watson [2001], channel forming-discharge, total stream power, or specific stream power) or in combination with a planform index. For 18 sites located in British Columbia and Alberta, Canada, Nandon and Hickin (1986) explained 70% of the variance of the volume of laterally eroded sediment from the outer banks using river size and grain size at the bank toe. In a regional analysis of migration rates of single-thread rivers mainly located in the Rhône River basin, France, Alber and Piégay (2017) explained 45% of the variability in migration rates using total stream power.

From a predictive and, thus, an operational point of view, one of the main drawbacks of the proposed models is that they cannot take into account the role of future hydrological variability, and, thus, the effects of ongoing climate change (Buffin-Bélanger et al., 2015). Long-term predictive values of retreat rates estimated through the logistic regression models could therefore be largely under- or overestimated depending on flood regime evolution. The only study dealing with evolution of the flood regime in the Loire Basin according to different climate change scenarios focused on maximum annual daily discharge with a 10-year return period (Moatar et al., 2010a, 2010b). Because of a too high level of uncertainty, it is impossible to predict future changes. Nevertheless, it is worth mentioning because lateral erosion on the Cher River is mainly controlled by low-magnitude events (Dépret et al., 2015), hence any changes in the occurrence frequency and/or duration of such common floods could strongly affect lateral mobility.

5.2 The issue of self-maintenance of river course migration

In this study, reaches with a significant shifting potential for preservation or restoration were located and prioritized (Figure 10). However, self-maintenance of mobility was not considered, even though it is a key influencer of the success of restoration operations (Kondolf, 2011). Self-maintenance is mainly dependent on sufficient bedload mobility and supply (Ahmed et al., 2019; Constantine et al., 2014; Donovan et al., 2021; Dunne et al., 2010). This supply, whether from upstream or from local reinjection resulting from bank erosion, promotes point bar fattening, which then increases tractive forces toward the opposite concave banks, ultimately sustaining lateral erosion processes (Dietrich and Smith, 1983, 1984; Dietrich et al., 1979; Legleiter et al., 2011). Local reinjection of coarse sediment following bank erosion is considered a major driver of lateral instability (Braudrick et al., 2009). This material is indeed partly redistributed onto the immediate downstream point bar (Pyrce and Ashmore, 2003a, 2003b, 2005), the development of which promotes lateral erosion on the opposite bank as previously explained. This creates a negative feedback loop, with bed migration maintained from near to far in the downstream direction. A reduction in coarse alluvial stock should thus be associated with a weakening of lateral erosive dynamics.

It was found that the Cher River could be separated into two sub-reaches with very distinct profiles in terms of the abundance of bars and alluvial riffles (Figure 3F). Whereas upstream of kp 73, bars and alluvial riffles are very frequent, they become very scarce downstream in favor of rocky riffles and bedrock reaches (Figure 3F). If we consider that this dichotomy reflects a marked difference in available bed-material load, and, thus, in bedload, and knowing that the specific stream power and curvature are not higher downstream (Figure 3C), it would be expected that the self-maintenance of the lateral erosion processes should be much more limited along the downstream sub-reach. This hypothesis would be confirmed, on the one hand, by retreat rates and the percentage of eroded river length from 1959 to 2016 that were significantly higher upstream of about kp 70 (Figure 3A and Figure 3B), and on the

723 other hand, by the percentage of river length with lateral constraints that does not increase
724 downstream (Figure 3E). Following this reasoning, restoration of lateral mobility by
725 removing bank protection would be less suitable on the downstream sub-reach.

726 This assumed lack of bedload in the downstream sub-reach could be the result of
727 excessive sediment mining in the riverbed from the 1960s to the 1980s (Dépret, 2014; Dépret
728 et al., 2021). However, these sediment extractions also were very significant in the upstream
729 sub-reach (Dépret, 2014). This explanation must, therefore, be at least partially rejected. The
730 lower availability of coarse sediment downstream could, thus, be due to inheritance, and be
731 explained by the decrease in the size and volume of coarse alluvium downstream. There is
732 evidence to support this postulation. First, the percentage of particles larger than 5 mm
733 (roughly the subsurface D_{50} (Dépret, 2014) in the alluvial infilling decreases significantly
734 from upstream to downstream. Above 40% between Montluçon and the Aumance junction
735 (from kp 0 to kp 37.1), it is ~25% at Saint-Amand-Montrond (kp 61.4), 15% at Châteauneuf-
736 sur-Cher (kp 88.85), 10% at Saint-Florent-sur-Cher (kp 108.8), and 5% at Brinay (kp 136.4),
737 slightly upstream of Vierzon (Figure 1) (BRGM-CETE de Lyon, 1979; Debrand-Passard et
738 al., 1977b; Turland et al., 1989c). A report on the survey of potential sand and gravel deposits
739 in the alluvial infill in the Cher River valley from Saint-Amand-Montrond also mentions a
740 fining of gravel between Saint-Amand-Montrond and Vierzon (kp 61.4 and 145.7) (Bos and
741 Trautmann, 1970). A similar downstream trend would apply to the thickness of coarse
742 sediment. The findings of another study aimed at identifying deposits of exploitable
743 aggregates in the alluvial plain of the Cher (CETE of Rouen, 1972) provide information in
744 particular, on the average thickness of coarse alluvium between La Perche (kp 45.55) and
745 Saint-Florent-sur-Cher (kp 108.8). Referred to as ‘gravelly sands’, their thickness would be
746 4.2 m between kp 45.55 and 55, 4.1 m between kp 55 and 69, 3.6 m between kp 69 and 87,
747 and 2.3 m between kp 87 and 105.2. These data tend to confirm the existence of a relatively

limited coarse alluvial stock in the downstream sub-reach. For this reason, riverbed mining could have had a greater impact here than in the upstream sub-reach. More broadly, this reduced stock of coarse sediment limits the reinjection of coarse sediments into the riverbed following bank erosion, with a consequent limited capacity for self-maintenance of lateral bed instability compared to the upstream sub-reach.

On the Cher River, the mechanisms for self-maintenance of bed migration dynamics also are most likely partially impeded due to livestock access to the riverbed. Along the study area, most of the proximal alluvial plain surface is devoted to sheep or cattle grazing. This has the effect of inhibiting or even preventing the development of vegetation on convex bars. Yet, such vegetation encroachment processes promote concave bank erosion (Bywater-Reyes et al., 2018; Zen and Perona, 2020). Thus, free access of livestock to the river likely diminishes lateral mobility of the Cher River.

Finally, regarding the removal of bank protections, one of the main uncertainties regarding the morphological evolution of sections relies on the sustainability of erosive activity. Such management actions would imply bed widening, and thus a likely decrease in specific stream power that could in turn lead to a decrease in the potential for lateral erosion.

5.3 Lateral constraints, sediment connectivity and lateral mobility

The mean and median length of constrained and unconstrained concave bank reaches were calculated to be 224–150 m and 255–150 m, respectively, hence decadal-scale bedload displacement velocities would be between 30 and 300 m per decade (Dépret et al., 2021). This means that coarse sediment connectivity between successive unconstrained reaches would likely be very limited, if not absent, at the decadal or even multi-decadal scale. This also implies that at this timescale, sediment reinjected into the bed by lateral erosion in a given unconstrained reach would not be deposited along the unconstrained reach immediately

downstream, and, would, therefore contribute little or nothing to the downstream maintenance of lateral dynamics. Furthermore, whereas lateral constraints, particularly bank protection, obviously prevent lateral erosion on reaches along which they are present, they would also indirectly limit the intensity of lateral erosion on reaches along which they are absent by reducing the sediment supply.

5.4 Prospects for improving the ecological status of the Cher River

Along the study reach, the ecological status of the river according to the WFD reference is considered poor upstream of the confluence with the Aumance River and moderate downstream (https://qualite-riviere.lesagencesdeleau.fr/; Figure 1). However, the WFD requires that good ecological status be reached. In the context of general coarse sediment starvation in rivers, resulting in damaged ecological functioning, river restoration strategies aimed at increasing the coarse sediment supply either by gravel augmentation or trough re-establishing space for channel shifting are becoming more popular (e.g., Arnaud et al., 2017; Bravard et al., 1999; Biron et al., 2014; Gaeuman, 2012; Kondolf, 2011; Rheinheimer and Yarnell, 2017; Rinaldi et al., 2011, Staenzel et al., 2020; Williams et al., 2020). Such actions promote longitudinal and cross-wise topographic as well as grain size heterogeneity, both of which increase the diversity of habitat, particularly aquatic habitat (Gaeuman, 2012; Yarnell et al., 2006; Hauer et al., 2018; Staenzel et al., 2020). Moreover, shifting riverscape mosaic processes caused by lateral mobility of rivers facilitates riparian succession associated with pulse disturbance (e.g., Diaz-Redondo et al., 2018; Gonzalez del Tanago et al., 2021; Hauer et al., 2016; Stanford et al., 2005; Tockner et al., 2010).

If it is assumed that the unsatisfactory ecological status of the Cher River is at least partly the result of the strong direct anthropogenic constraints exerted on the lateral mobility of the river, no improvement in ecological status is likely to be achieved without restoration

of this mobility. However, it has been revealed that such restoration only concerns a relatively limited number of sections (Figure 10). Furthermore, the low bedload velocity (Section 5.3) indicates that most of the coarse sediment reinjected in the riverbed by lateral erosion would remain at a decadal scale in close proximity to the eroded banks. This implies that only a local increase in the heterogeneity of aquatic and riparian habitat could be achieved through such injections. The effects of management actions aimed at restoring lateral mobility would, thus, be spatially limited. Therefore, questions remain to what extent such local diversification could impact the biodiversity of constrained sections located upstream and downstream of restored sections. With this in mind, there appears to be little possibility of achieving good ecological status along the entire length of the river through removal of bank protection. Furthermore, uncertainty remains on the timescale needed for the morphological effects of the removal of protections to be felt. Because the erosive process is relatively slow it could take several years, or even longer, before these actions achieve the desired effect. Such a time-scale does not comply with the needs of managers to obtain ecological improvements in the short term. Due to these spatial and temporal limitations, it might be more productive to implement a combination of rip-rap removal with a series of gravel augmentations close to each other.

5.5 Applicability and reproducibility of the method for meandering gravel-bed rivers

The main principles guiding our methodological approach involve some key elements of previous work through which are identified and delineated the alluvial plain, the historical trajectory of the river course, the zone potentially prone to lateral erosion in the near future (upcoming decades), as well as SEIs in order to preserve an erodible corridor in the alluvial plain (e.g., Malavoi et al., 1998; Piégay et al., 1997, 2005; Biron et al., 2014). However, our methodological framework differs from these previous studies; in addition to enabling the

detection of river sections along which bank erosion, and thus an erodible corridor, could be preserved, it also focuses on whether and where lateral mobility could be restored. The different steps of the method, replicable regardless of the energy of meandering gravel-bed rivers, are (1) assessment of bed mobility over recent decades; (2) identification of the lateral constraints (natural and anthropogenic) to lateral mobility and SEIs in the floodplain; (3) quantification and location of their effects on the available space for river shifting; (4) determination of the relationship (through regression) between retreat rates and their controlling factors along river sections without constraints; (5) delimitation of sections where lateral constraints could be removed; (6) application of the regression developed in step 4 to reaches identified in step 5; (7) prioritisation of preservation and restoration sections according to a combination of criteria defined in accordance with river managers (i.e., predicted retreat rates, length of river sections, and width of the remaining space for river shifting).

This approach, when applied alongside information on bedload transport and availability, could facilitate defining the most suitable and sustainable restoration actions in terms of sediment budgeting and sediment exchanges between the river and its floodplain. Along any river corridor, three management options are available and can be combined depending on the intensity of constraints and SEIs, and the potential of the river for lateral mobility: removal of constraints, gravel augmentation, and combining these two. While all three options are suitable in the case of sediment starvation, and thus enable the enhancement of aquatic habitats (e.g., Chardon et al., 2021; Mörtl and De Cesare, 2021), removal of lateral constraints is the only measure that simultaneously promotes the improvement of riparian habitats (e.g., Larsen et al., 2006). For this reason, removal of lateral constraints is thus a relevant management action regardless the existence of any sediment deficit. More broadly, such removal is also directly related to other issues since it can promote, for instance, a local

and downstream reduction in flood hazard by increasing water storage in the floodplain during high-flow periods (Arnaud-Fassetta et al., 2009; Benito and Vázquez-Tarrío, 2022). Finally, the robustness of our approach could be enhanced by integrating into the erodible corridor different flooding zones as proposed by Biron et al. (2014) in their definition of freedom space, since the ecological integrity of rivers is also governed by maintenance of the surface and subsurface hydrological connectivity between riverbed and floodplain (Amoros and Bornette, 2002).

6. Conclusions

The results of the current study allowed the very strong fragmentation of the Cher River to be highlighted and quantified. Most of the river is laterally constrained due to the presence of anthropogenic structures such as bank protection, former gravel pits in the alluvial plain, bridges, and weirs. Today, the Cher River is composed of a string of constrained and unconstrained reaches, and its available space for channel shifting has been strongly reduced. Because of the fluvial engineering works and anthropogenic legacies, most of the potential for lateral movement of the riverbed, and, therefore, diversification of the riparian and aquatic habitat, has been lost. Due 1) to the very low proportion of the river length with lateral mobility that could be preserved or restored, such restoration can only be done by removal of bank protection where possible, 2) to the very likely local effects of restoration of the lateral mobility, and assuming that the unsatisfactory ecological status of the Cher River is at least partly the result of the strong, direct anthropogenic constraints exerted on the lateral mobility of the river, the probability that a good ecological status can be achieved along the entire river length by removal of bank protection is very low. For these different reasons, implementation of rip-rap removal combined with a series of gravel augmentations close to each other could help toward achieving good ecological status along the entire length of the Cher River.

This research has expanded the understanding of how the morpho-sedimentary functioning of a low-energy, gravel-bed river can be impaired by current and past direct anthropogenic constraints, and how to determine the river's recovery potential. However, characterizing the factors controlling the diversity of biotopes and biocenoses through the hydrosedimentary dynamics of such rivers remains challenging. On these rivers, and unlike high-energy rivers, morphogenic processes occur at a relatively reduced intensity and at moderate velocities. For this reason, the effects of direct anthropogenic constraints on the degree of habitat heterogeneity and biodiversity may be much less pronounced than for high-energy rivers. Conversely, the morpho-sedimentary response time of the system to the removal of these constraints could be relatively long. The links between alteration of hydrosedimentary dynamics and biotope degradation, therefore, require further clarification.

Acknowledgements

The current research was done within the framework of the *Plan Loire Grandeur Nature*. It was funded by the European Regional Development Fund *Bassin de la Loire* and the *Agence de l'Eau Loire-Bretagne*. The authors thank Dominique Dépret and Bruno Dépret for their invaluable help in the field survey, and Lise Vaudor for her assistance with logistic regression. Finally, the authors are very grateful to the editor and the two reviewers for their very helpful comments that greatly improved the overall quality of the paper.

References

Ahmed, J., Constantine, J.A., Dunne, T., 2019. The role of sediment supply in the adjustment of channel sinuosity across the Amazon Basin. Geology 47 (9), 807–810.

Alber, A., Piégay, H., 2017. Characterizing and modelling river channel migration rates at a regional scale: Case study of south-east France. J. Environ. Manage. 202 (2), 479–493.

Amoros, C., Bornette, G., 2002. Connectivity and biocomplexity in waterbodies of riverine floodplains. Freshwater Biology 47, 761–776.

Arnaud, F., Piégay, H., Béal, D., Collery, P., Vaudor, L., Rollet, A.J., 2017. Monitoring gravel augmentation in a large regulated river and implications for process-based restoration. Earth Surf. Process. Landf. 42 (13), 2147–2166.

Arnaud-Fassetta, G., Astrade, L., Bardou, E., Corbonnois, J., Delahaye, D., Fort, M., Gautier, E., Jacob, N., Peiry, J.L., Piégay, H., Penven, M.J., 2009. Fluvial geomorphology and flood-risk management. Géomorphologie : relief, processus, environnement 15 (2), 109–128.

Baudrick, C.A., Dietrich, W.E., Leverich, G.T., Sklar, L.S., 2009. Experimental evidence for the conditions necessary to sustain meandering in coarse-bedded rivers. Proc. Natl. Acad. Sci. U.S.A. 106 (40), 16936–16941.

Basak, S.M., Hossain, M.S., Tusznio, J., Grodzińska-Jurczak, M., 2021. Social benefits of river restoration from ecosystem services perspective: A systematic review. Environ. Sci. Policy 124, 90–100.

Beechie, T.J., Sear, D.A., Olden, J.D., Pess, G.R., Buffington, J.M., Moir, H., Roni, P., Pollock, M.M., 2010. Process-based Principles for Restoring River Ecosystems. BioScience 60 (3), 209–222.

Benito, G., Vázquez-Tarrío, D., 2022. Hazardous Processes: Flooding. In Shroder, J.F., James, A., Harden, C.P., and Clague, J.J., (Eds.), Treatise on Geomorphology, Anthropogenic Geomorphology, Edition 2, Chapter 9.30. Academic PressEditors, pp. 715–743.

Biron, P.M., Buffin-Bélanger, T., Larocque, M., Choné, G., Cloutier, C.A., Ouellet, M.A., Demers, S., Olsen, T., Desjarlais, C., Eyquem, J., 2014. Freedom Space for Rivers: A Sustainable Management Approach to Enhance River Resilience. Environ. Manage. 54, 1056–1073.

Bledsoe, B.P., Watson, C.C., 2001. Logistic regression of channel pattern thresholds: meandering, braiding and incising. Geomorphology 38, 281–300.

Bogoni, M., Putti, M., Lanzoni, S., 2017. Modeling meander morphodynamics over self-formed heterogeneous floodplains. Water Resour. Res. 53 (6), 5137–5157.

Borgwardt, F., Robinson, L., Trauner, D., Teixeira, H., Nogueira, A.J.A., Lillebø, A.I., Piet, G., Kuemmerlen, M., O'Higgins, T., McDonald, H., Arevalo-Torres, J., Barbosa, A.L., Iglesias-Campo, A., Hein, T., Culhane, F., 2019. Exploring variability in environmental impact risk from human activities across aquatic ecosystems. Sci. Total Environ. 660, 611–621.

Bos, P., Trautman, F., 1970. Etude des gisements potentiels de sables et graviers de la vallée du Cher de Saint-Amand-Montrond (Cher) au confluent avec la Loire. BRGM.

Bravard, J.P., Landon, N., Peiry, J.L., Piégay, H., 1999. Principles of engineering geomorphology for managing channel erosion and bedload transport, examples from French rivers. Geomorphology 31, 291–311.

BRGM – CETE de Lyon, 1979. Synthèse et interaction des ressources en granulats et eaux souterraines dans la vallée du Cher et sur la zone granitique de Montluçon.

Brown, A.G., Lespez, L., Sear, D.A., Macaire, J.J., Houbend, P., Klimek, K., Brazier, R.E., Van Oost, K., Pears, B., 2018. Natural vs anthropogenic streams in Europe: History, ecology and implications for restoration, river-rewilding and riverine ecosystem services. Earth Sci. Rev. 180, 185–205.

947 Buffin-Bélanger, T., Biron, P.M., Larocque, M., Demers, S., Olsen, T., Choné, G., Ouellet,
948 M.A., Cloutier, C.A., Desjarlais, C., Eyqueme, J., 2015. Freedom space for rivers: An
949 economically viable river management concept in a changing climate. Geomorphology
950 251, 137–148.
951 Bywater-Reyes, S., Diehl, R.M., Wilcox, A.C., 2018. The influence of a vegetated bar on
952 channel-bend flow dynamics. Earth Surf. Dyn. 6, 487–503.
953 CETE de Rouen, 1972. Recherches de matériaux dans la vallée du Cher. Note technique.
954 Chardon, V., Schmitt, L., Arnaud, F., Piégay, H., Clutier, A., 2021. Efficiency and
955 sustainability of gravel augmentation to restore large regulated rivers: Insights from three
956 experiments on the Rhine River (France/Germany). Geomorphology, 107639.
957 Choné, G., Biron, P.M., 2016. Assessing the Relationship Between River Mobility and
958 Habitat. 32 (4), River Res. Appl. 528–539.
959 Ciotti, D.C., Mckee, J., Pope, K.L., Kondolf, G.M., Pollock, M.M., 2021. Design Criteria for
960 Process-Based Restoration of Fluvial Systems. BioScience 71 (8), 831–845.
961 Constantine, C.R., Dunne, T., Hanson, G.J., 2009. Examining the physical meaning of the
962 bank erosion coefficient used in meander migration modeling. Geomorphology 106,
963 242–252.
964 Constantine, J.A., Dunne, T., Ahmed, J., Legleiter, C., Lazarus, E.D., 2014. Sediment supply
965 as a driver of river meandering and floodplain evolution in the Amazon Basin. Nature
966 Geoscience 7, 899–903.
967 Cossalter, F., 2011. Des carrières alluviales aux captures dans la vallée du Cher. Analyses
968 spatiales et méthodes de mesures des impacts hydrologiques et sédimentaires. Master 2
969 thesis in Geography, Paris 1 Panthéon-Sorbonne University.
970 Cox, D.R., Snell, E.J., 1989. Analysis of Binary Data. Second Edition. Chapman & Hall.

971 Culhane, F., Teixeira. H., Nogueira, A.J.A., Borgwardt, F., Trauner, D., Lillebø, A., Piet, G.,
972 Kuemmerlen, M., McDonald, H., O'Higgins, T., Barbosa, A.L., van der Wal, J.T.,
973 Iglesias-Campos, A., Arevalo-Torres, J., Barbière, J., Robinson, L.A., 2019. Risk to the
974 supply of ecosystem services across aquatic ecosystems. Sci. Total Environ. 652, 1396–
975 1408.
976 Debrand-Passard, S., Lablanche, G., Flamand, D., Soulas, J.P., 1977a. Carte géol. France
977 (1/50000), feuille Bourges (519). Orléans : BRGM.
978 Debrand-Passard, S., Lablanche, G., Flamand, D., Soulas, J.P., 1977b. Notice explicative,
979 Carte géol. France (1/50000), feuille Bourges (519). Orléans : BRGM.
980 Debrand-Passard, S., Lablanche, G., Medioni, R., Flamand, D., Audebourg, B., Petitfils, B.,
981 Martin, B., 1978. Carte géol. France (1/50000), feuille Vatan (518). Orléans : BRGM.
982 Dépret, T., 2014. Fonctionnement morphodynamique actuel et historique des méandres du
983 Cher. Ph. Thesis, Paris 1 Panthéon-Sorbonne University.
984 Dépret, T., 2021. READED. Réajustements morpho-sédimentaires du Cher aux contraintes
985 anthropiques actuelles et passées. Résilience et perspectives de restauration. Rapport
986 final & recommandations opérationnalles, 93 p.
987 Dépret, T., Gautier, E., Hooke, J., Grancher, D., Virmoux, C., Brunstein, D., 2015.
988 Hydrological controls on the morphogenesis of low-energy meanders (Cher River,
989 France). J. Hydrol. 531, 877–891.
990 Dépret, T., Gautier, E., Virmoux, C., Gob, F., Piégay, H., Mesmin, E., Doncheva, M.,
991 Plaisant, B., Ghamgui, S., Clocet, O., Peyret, A., 2021. READED - Réajustements
992 morpho-sédimentaires du Cher aux contraintes anthropiques actuelles et passées,
993 Résilience et perspectives de restauration. Rapport final et recommandations
994 opérationnelles. Rapport (95 pp.).Dépret, T., Gautier, E., Hooke, J., Grancher, D.,

995 Virmoux, C., Brunstein, D., 2017. Causes of planform stability of a low-energy
996 meandering gravel-bed river (Cher River, France). Geomorphology 285, 58–81.
997 Diaz-Redondo, M., Marchamalo, M., Egger, G., Magdaleno, F., 2018. Toward floodplain
998 rejuvenation in the middle Ebro River (Spain): From history to action. Geomorphology
999 317, 117–127.
1000 Dietrich W.E., Smith J.D., 1983. Influence of the Point Bar on Flow Through Curved
1001 Channels. Water Resour. Res. 19 (5), 1173–1192.
1002 Dietrich, W.E., Smith, J.D., 1984. Bed load transport in a river meander. Water Resour. Res.
1003 20 (10), 1355–1380.
1004 Dietrich W.E., Smith J.D., Dunne T., 1979. Flow and sediment transport in a sand bedded
1005 meander. J. Geol. 87, 305–315.
1006 Donovan, M., Belmont, P., Sylvester, Z., 2021. Evaluating the relationship between meander-
1007 bend curvature, sediment supply, and migration rates. J. Geophys. Res. Earth. Surf., 126,
1008 e2020JF006058.
1009 Downs, P.W., Gregory, K.J., 2004. River Channel Management: Towards Sustainable
1010 Catchment Hydrosystems. London: Arnold, 408 p.
1011 Downs, P.W., Piégay, H., 2019. Catchment-scale cumulative impact of human activities on
1012 river channels in the late Anthropocene: implications, limitations, prospect.
1013 Geomorphology 338, 88–104.
1014 Dudgeon, D., 2019. Multiple threats imperil freshwater biodiversity in the Anthropocene.
1015 Curr. Biol. 29 (19), R960–R967.
1016 Dudgeon, D., Arthington, A.H., Gessner M.O., Kawabata, Z.I., Knowler, D.J., Lévêque, C.,
1017 Naiman, R.J., Prieur-Richard, A.H., Soto, D., Stiassny, M.L.J., Sullivan, C.A., 2006.
1018 Freshwater biodiversity: importance, threats, status and conservation challenges. Biol.
1019 Rev. 81 (2), 163–182.

Dunne, T., Constantine, J.A., Singer, M.B., 2010. The role of sediment transport and sediment supply in the evolution of river channel and floodplain complexity. Trans. Jpn. Geomorphol. Union 31 (2), 155–170.

Ekka, A., Pande, S., Jiang, Y., van der Zaag, P., 2020. Anthropogenic Modifications and River Ecosystem Services: A Landscape Perspective. Waters 12, 2706.

Elosegi, A., Díez, J., Mutz, M., 2010. Effects of hydromorphological integrity on biodiversity and functioning of river ecosystems. Hydrobiologia 657, 199–215.

European Parliament and Council, 2000. Directive 2000/60/EC establishing a framework for community action in the field of water policy. Official Journal of the European Union L 327, 22.12.2000.

Fisk, H.N., 1944. Geological investigation of the alluvial valley of the lower Mississippi River. U.S. Army Corps of Engineers, Mississippi River Commission, Vicksburg, 78 p.

Fisk, H.N., 1947, Fine-grained alluvial deposits and their effect on Mississippi River activity: Vicksburg, Mississippi. U.S. Army Corps of Engineers, Mississippi River Commission, Vicksburg, 82 p.

Florsheim, J.L., Mount, J.F., Chin, A., 2008. Bank erosion as a desirable attribute of rivers. BioScience 58 (6), 519–529.

Fremier, A.K., Girvetz, E.H., Greco, S.E., Larsen, E.W., 2014. Quantifying Process-Based Mitigation Strategies in Historical Context: Separating Multiple Cumulative Effects on River Meander Migration. PLoS One 9 (6), e99736.

Friedman, J.M., Osterkamp, W.R., Scott, M.L., Auble, G.T., 1998. Downstream effects of dams on channel geometry and bottomland vegetation: regional patterns in the Great Plains. Wetlands 18 (4), 619–633.

Fryirs, K.A., 2017. River sensitivity: a lost foundation concept in fluvial geomorphology. Earth Surf. Process. Landf. 42 (1), 55–70.

1045 Fryirs, K.A., Brierley, G.J., 2016. Assessing the geomorphic recovery potential of rivers:
1046 forecasting future trajectories of adjustment for use in management. WIREs Water 3,
1047 727–748.
1048 Fryirs, K.A., Brierley, G.J., in press. How far have management practices come in 'working
1049 with the river'? Earth Surf. Process. Landf.
1050 Fryirs, K.A., Wheaton, J.M., Brierley, G.J., 2016. An approach for measuring confinement
1051 and assessing the influence of valley setting on river forms and processes. Earth Surf.
1052 Process. Landf. 41 (5), 701–710.
1053 Furbish, D.J., 1988. River-bend curvature and migration – How are they related. Geology 16
1054 (8), 752–755.
1055 Gaeuman, D.A., 2012. Mitigating downstream effects of dams. In: Church, M., Biron, P.,
1056 Roy, A.G. (Eds.), Gravel-bed Rivers: Processes, Tools, Environments. John Wiley &
1057 Sons, Chichester, pp. 182–189.
1058 Gaueman, D.A., Schmidt, J.C., Wilcock, P.R., 2003. Evaluation of in-channel gravel storage
1059 with morphology-based gravel budgets developed from planimetric data. J. Geophys.
1060 Res. 108 (F1), 6001.
1061 González del Tánago, M., Martínez-Fernández, V., Aguiar, F.C., Bertoldi, W., Dufour, S.,
1062 García de Jalón, D., Garófano-Gómez, V., Mandzukovski, D., Rodríguez-González,
1063 P.M., 2021. Improving river hydromorphological assessment through better integration
1064 of riparian vegetation: Scientific evidence and guidelines. J. Environ. Manage. 292,
1065 112730.
1066 Grizzetti, B., Pistocchi, A., Liquete, C., Udias, A., Bouraoui, F., van de Bund, W., 2017.
1067 Human pressures and ecological status of European rivers. Scientific Reports 7, 205.
1068 Güneralp, I., Rhoades, B.L., 2011. Influence of floodplain erosional heterogeneity on
1069 planform complexity of meandering rivers. J. Geophys. Res. 38, L14401.

Gurnell, A.M., Downward, S.R., Jones, R., 1994. Channel planform change on the River Dee meanders, 1876–1992. River Res. Appl. 9 (4), 187–204.

Hauer, C., Leitner, P., Unfer, G., Pulg, U., Habersack, H., Graf, W., 2018. The Role of Sediment and Sediment Dynamics in the Aquatic Environment. In: Schmutz, S., Sendzimir, J. (Eds.), Riverine Ecosystem Management. Aquatic Ecology Series, vol 8. Springer, Cham, pp 151–169.

Hauer, F.R., Locke, H., Dreitz, V.J., Hebblewhite, M., Lowe, W.H.,Muhfield, C.C., Nelson, C.R., Proctor, M.F., Rood, S.B., 2016. Gravel-bed river floodplains are the ecological nexus of glaciated mountain landscapes. Science Advances 2 (6), e1600026.

Hoffmann, T., 2015. Sediment residence time and connectivity in non-equilibrium and transient geomorphic systems. Earth Sci. Rev. 150, 609–627.

Hoffmann, T., Thorndycraft, V.R., Brown, A.G., Coulthard, T.J., Damnati, B., Kale, V.S., Middelkoop, H., Notebaert, B., Walling, D.E., 2010. Human impact on fluvial regimes and sediment flux during the Holocene: Review and future research agenda. Glob. Planet. Change 72, 87–98.

Horton, A.J., Constantine, J.A., Hales, T.C., Goossens, B., Bruford, M.W., Lazarus, E.D., 2017. Modification of river meandering by tropical deforestation. Geology 45 (6), 511–514.

Hubert, P., 2000. The segmentation procedure as a tool for discrete modeling of hydrometeorological regimes. Stochastic Environmental Research and Risk Assessment 14, 297–304.

Hubert, P., Carbonnel, J.P., Chaouche, A., 1989. Segmentation des séries hydrométéorologiques — application à des séries de précipitations et de débits de l'afrique de l'ouest. Journal of Hydrology 110, 349–367.

Ielpi, A., Lapôtre, M.G.A., 2020. A tenfold slowdown in river meander migration driven by plant life. Nature Geoscience 13, pages 82–86.

IGN, 2016. BD Ortho version 2.0, Ortho HR version 1.0, Descriptif de contenu.

Khan, S., Fryirs, K.A., 2020. An approach for assessing geomorphic river sensitivity across a catchment based on analysis of historical capacity for adjustment. Geomorphology 359, 107135.

Kondolf, M.G., 2011. Setting Goals in River Restoration: When and Where Can the River "Heal Itself"? In: Bennett, S.J., Castro, J.M., Simon, A. (Eds.), Stream Restoration in Dynamic Fluvial Systems: Scientific Approaches, Analyses, and Tools. Geophysical Monograph 194, American Geophysical Union, pp. 29–43.

Lablanche, G., 1984. Carte géol. France (1/50000), feuille Châteauneuf-sur-Cher (546), BRGM, Orléans.

Lablanche, G., 1994. Carte géol. France (1/50000), feuille Saint-Amand-Montrond (572), BRGM, Orléans.

Lablanche, G., Marchand, D., Lefavarais-Raymond, A., Debrand-Passard, S., Gros, Y., Debéglia, N., Maget, P., Lallier, D., 1994. Notice explicative, Carte géol. France (1/50000), feuille Saint-Amand-Montrond (572), BRGM, Orléans, 81 p.

Larsen, E.W., Girvetz, E.H., Fremier, A.K., 2006. Assessing the Effects of Alternative Setback Channel Constraint Scenarios Employing a River Meander Migration Model. Environ. Manage. 37, 880–897.

Larue, J.P., 1981. Les nappes alluviales de la vallée du Cher dans le bassin de Montluçon. Norois 111, 345–360.

Larue, J.P., 1994. L'évolution morphodynamique de la vallée du Cher dans la région de Saint-Amand-Montrond (Cher, France). Rev. Géomorphol. Dynam. 43 (3), 81–92.

1118 Larue, J.P., 2011. Longitudinal profiles and knickzones: the example of the rivers of the Cher
1119 basin in the northern French Massif Central. Proc. Geol. Assoc. 122, 125–142.
1120 Legleiter, C.J., Harrison, L.R., Dunne, T., 2011. Effect of point bar development on the local
1121 force balance governing flow in a simple, meandering gravel bed river. J. Geophys. Res.
1122 116, F01005.
1123 Lehner, B., Reidy Liermann, C., Revenga, C., Vörösmarty, C., Fekete, B., Crouzet, P., Döll,
1124 P., Endejan, M., Frenken, K., Magome, J., Nilsson, C., Robertson, J.C., Rödel, R.,
1125 Sindorf, N., Wisser, D., 2011. High-resolution mapping of the world's reservoirs and
1126 dams for sustainable river-flow management. Front. Ecol. Environ. 9 (9), 494–502.
1127 Maaß, A.L., Schüttrumpf, H., Lehmkuhl, F., 2021. Human impact on fluvial systems in
1128 Europe with special regard to today's river restorations. Environ. Sci. Eur. 33, 119.
1129 Malavoi, J.R., Bravard, J.P., Piégay, H., Hérouin, E., Ramez, P., 1998. Détermination de
1130 l'espace de liberté des cours d'eau. Guide technique no. 2, SDAGE RMC.
1131 Manivit, J., Debrand-Passard, S., 1994. Carte géol. France (1/50000), feuille Vierzon (491),
1132 BRGM, Orléans.
1133 Manivit, J., Debrand-Passard, S., Gros, Y., Desprez, N., 1994. Notice explicative, Carte géol.
1134 France (1/50000), feuille Vierzon (491), BRGM, Orléans, 50 p.
1135 Micheli, E.R., Kirchner, J.W., 2002. Effects of wet meadow riparian vegetation on
1136 streambank erosion. 1. Remote sensing measurements of streambank migration
1137 erodibility. Earth Surf. Process. Landf. 27, 627–639.
1138 Micheli E.R., Kirchner J.W., Larsen E.W., 2004. Quantifying the effect of riparian forest
1139 versus agricultural vegetation on river meander migration rates, central Sacramento
1140 River, California, USA. River Res. Appl. 20, 537–548.
1141 Moatar, F., Ducharne, A., Thiéry, D., Bustillo, V., Sauquet, E., Vidal, J.P., 2010. La Loire à
1142 l'épreuve du changement climatique. Géosciences BRGM 12, 78–87.

Moatar, F., Ducharne, A., Thiéry, D., Sauquet, E., Vidal, J.P., Bernard, A., Bustillo, V., 2010. Impact du Changement Climatique sur l'hydrosystème Loire : HYDROlogie, Régime thermique, QUALité des eaux. Action 1 : Evolution hydroclimatique de la Loire et de ses affluents sous changement climatique. Rapport final, 105 p.

Mörtl, C., De Cesare, G., 2021. Sediment Augmentation for River Rehabilitation and Management—A Review. Land 10, 1309.

Motta, D., Abad, J.D., Langendoen, E.J., Garcia, M.H., 2012. The effects of floodplain soil heterogeneity on meander planform shape. Water Resour. Res. 48, W09518.

Nanson, G.C., Kickin, E.J., 1986. A statistical analysis of bank erosion and channel migration in western Canada. Geol. Soc. Am. Bull. 97, 497–504

Notebaert, B., Verstraeten, G., 2010. Sensitivity of West and Central European river systems to environmental changes during the Holocene: A review. Earth Sci. Rev. 103, 163–182.

Obert, D., Gély, J.P., Mathis, V., Normand, M., Trouillet, A., Freytet, P., 1997. Carte géol. France (1/50000), feuille Charenton-sur-Cher (573). Orléans : BRGM.

Overeem, I., Kettner, A.J., Syvitski, J., 2013. Impacts of Humans on River Fluxes and Morphology. In Shroder, J.F., Wohl E., (Eds.), Treatise on Geomorphology, Fluvial Geomorphology, Edition 1, Chapter 9.40. Academic PressEditors, pp. 828–842.

Piégay, H., Arnaud, D., Souchon, Y., 2003. Effets de la végétation riveraine sur la géométrie des lits fluviaux : études de cas dans le Massif central (France). Geomorphol. Relief, Process. Environ. 9 (2), 111–127.

Piégay, H., Cuaz, M., Javelle, E., Mandier, P., 1997. Bank erosion management based on geomorphological, ecological and economic criteria on the Galaure River, France. River Res. Appl. 13 (5), 433–448.

Piégay, H., Darby, S.E., Mosselman, E., Surian, N., 2005. A review of techniques available for delimiting the erodible river corridor: a sustainable approach to managing bank erosion. River Res. Appl. 21 (7), 773–789.

Pyrce, R.S., Ashmore, P.E., 2003a. The relation between particle path length distributions and channel morphology in gravel-bed streams: A synthesis. Geomorphology 56, 167–187.

Pyrce, R.S., Ashmore, P.E., 2003b. Particle path length distributions in meandering gravel-bed streams: Results from physical models. Earth Surf. Process. Landf. 28, 951–966.

Pyrce, R.S., Ashmore, P.E., 2005. Bedload path length and point bar development in gravel-bed river models. Sedimentology 52, 839–857.

Reid, D., Church, M., 2015. Geomorphic and Ecological Consequences of Riprap Placement in River Systems. J. Am. Water. Resour. Assoc. 51 (4), 1043–1059.

Reid, H.E., Brierley, G.J., 2015. Assessing geomorphic sensitivity in relation to river capacity for adjustment. Geomorphology 251, 108–121.

Rheinheimer, D.E., Yarnell, S.M., 2017.Tools for sediment management in rivers. In: Horne, A.C., Webb, J.A., Stewardson, M.J., Richter, B., Acreman, M. (Eds.), Water for the Environment, from Policy and Science to Implementation and Management. Academic Press, pp. 237–263.

Richard, G.A, Julien, P.Y., Baird, D.C., 2005. Statistical analysis of lateral migration of the Rio Grande, New Mexico. Geomorphology 71, 139–155.Rigby, R. A., Stasinopoulos, D.M., 2005. Generalized additive models for location, scale and shape (with discussion). Applied Statistics 54, 507–554.

Rinaldi, M., Piégay, H., Surian, N., 2011. Geomorphological Approaches for River Management and Restoration in Italian and French Rivers. In: Bennett, S.J., Castro, J.M., Simon, A. (Eds.), Stream Restoration in Dynamic Fluvial Systems: Scientific

Approaches, Analyses, and Tools. Geophysical Monograph 194, American Geophysical Union, pp. 319–336.

Rinaldi, M., Wyżga, B., Surian, N., 2005. Sediment mining in alluvial channels: physical effects and management perspectives. River Res. Appl. 21 (7), 805–828.

Rollet, A.J., Piégay, H., 2013. De l'intérêt de la quantification pour la gestion des systèmes fluviaux : exemple de la basse vallée de l'Ain. Geomorphol. Relief, Process. Environ. 1, 63–78.

Roux, C., Alber, A., Bertrand, M. Vaudor, L., Piégay, H., 2015. "FluvialCorridor": A new ArcGIS toolbox package for multiscale riverscape exploration. Geomorphology 242, 29–37.

Schumm, S.A., Harvey, M.D., Watson, C.C., 1984. Incised channels: Morphology, dynamics, and control, Water Resources Publications, Littleton, Colorado, 200 p.

Simon, A., 1989. A model of channel response in disturbed alluvial channels. Earth Surf. Process. Landf. 14, 11–26.

Simon, A., Rinaldi, M., 2006. Disturbance, stream incision, and channel evolution: The roles of excess transport capacity and boundary materials in controlling channel response. Geomorphology 79, 361–383.

Simon-Coinçon, R., Thiry, M., Quesnel, F., 2000. Paléopaysages et paléoenvironnements sidérolithiques du Nord du Massif central (France). C. R. Acad. Sci. Ser. IIA Earth Planet. Sci. 330, 693–700.

Staenzel, C., Kondolf, M., Schmitt, L., Combroux, I., Barillier, A., Beisel, J.N., 2020. Restoring fluvial forms and processes by gravel augmentation or bank erosion below dams: A systematic review of ecological responses. Sci. Total Environ. 706, 135743.

Stanford, J.A., Lorang, M.S., Hauer, F.R., 2005. The shifting habitat mosaic of river ecosystems. Verh. Int. Ver. Theor. Angew. Limnol. 29 (1), 123-136.

Surian, N., 2021. Fluvial Changes in the Anthropocene: A European Perspective. In: Elias, S.A. (Eds.), Reference Module in Earth Systems and Environmental Sciences. Elsevier, Amsterdam.

Sylvester, Z., Durkin, P., Covault, J.A., 2019. High curvatures drive river meandering. Geology 47, 263–266.

Taylor, J., 1997. An Introduction to Error Analysis: The Study of Uncertainties in Physical Measurements. University Science Books, Sausalito, California.

Tockner, K., Lorang, M.S., Stanford, J.A., 2010. River flood plains are model ecosystems to test general hydrogeomorphic and ecological concepts. River Res. Appl. 26, 76-86.

Turland, M., Cojean, R., Brulhet, J., Morice, E., Grolier, J., Lacour, A., 1989a. Carte géol. France (1/50000), feuille Hérisson (596), BRGM, Orléans.

Turland, M., Feys, R., Desthieux, F., Virlogeux, D., 1989b. Carte géol. France (1/50000), feuille Montluçon (619), BRGM, Orléans.

Turland, M., Hottin, A.M., Cojean, R., Ducreux, J.L., Debéglia, N., d'Arcy, D., Mathis, V., Carroué, J.P., Piboule, M., 1989c. Notice explicative, Carte géol. France (1/50000), feuille Hérisson (596), BRGM, Orléans, 118 p.

Vayssière,A., Dépret, T., Castanet,C.,Gautier,E.,Virmoux,C., Carcaud, N.,Garnier,A., Brunstein, D., Pinheiro, D., 2016. Etude des paléoméandres holocènes de la plaine alluviale du Cher (site de Bigny, moyenne vallée du Cher). Geomorphol. Relief, Process. Environ. 22 (2), 163–176.

Vayssière, A., Castanet, C., Gautier, E., Virmoux, C., Dépret, T., Gandouin, E., Develle-Vicent, A.L., Mokadem, F., Saulnier-Copard, S., Sabatier, P., Carcaud N., 2020. Long-term readjustments of a sinuous river during the second half of the Holocene in northwestern Europe (Cher River, France). Geomorphology 370.

1239 Vörösmarty, C.J., McIntyre, P.B., Gessner, M.O., Dudgeon, D., Prusevich, A., Green, P.,
1240 Glidden, S., Bunn, S.E., Sullivan, C.A., Reidy Liermann, C., Davies, P.M., 2010. Global
1241 threats to human water security and river biodiversity. Nature 467, 555–561.
1242 Watson, C.C., Biedenharn, D.S., Bledsoe, B.P., 2002. Use of incised channel evolution
1243 models in understanding rehabilitation alternatives. J. Am. Water Resour. Assoc. 38 (1),
1244 151–160.
1245 Williams, R.D., Bangen, S., Gillies, E., Kramer, N., Moir, H., Wheaton, J., 2020. Let the river
1246 erode! Enabling lateral migration increases geomorphic unit diversity. Sci. Total
1247 Environ. 715, 136817.
1248 Wohl E., 2020. Rivers in the Anthropocene: The U.S. perspective. Geomorphology 366,
1249 106600.
1250 Yarnell, S.M., Mount, J.F., Larsen, E.W., 2006. The influence of relative sediment supply on
1251 riverine habitat heterogeneity. Geomorphology 80, 310–324.
1252 Zen, S., Perona, P., 2020. Biomorphodynamics of river banks in vegetated channels with self-
1253 formed width. Adv. Water Resour. 135, 103488.